The Effect of Multiple Time Scales and Subexponentiality in MPEG Video Streams on Queueing Behavior

Predrag R. Jelenković, *Associate Member, IEEE*, Aurel A. Lazar, *Fellow, IEEE*, and Nemo Semret

***Abstract*— Guided by the empirical observation that real-time MPEG video streams exhibit both multiple time scale and subexponential characteristics, we construct a video model that captures both of these characteristics and is amenable to queueing analysis. We investigate two fundamental approaches for extracting the model parameters: using sample path and second-order statistics-based methods. The model exhibits the following two canonical queueing behaviors.**

When *strict stability* conditions are satisfied, i.e., the conditional mean of each scene is smaller than the capacity of the server, precise modeling of the interscene dynamics (long-term dependency) is not essential for the accurate prediction of small to moderately large queue sizes. In this case, the queue length distribution is determined using quasistationary (perturbation theory) analysis.

When *weak stability* conditions are satisfied, i.e., the conditional mean of at least one scene type is greater than the capacity of the server, the dominant effect for building a large queue size is the subexponential (long-tailed) scene length distribution. In this case, precise modeling of intrascene statistics is of secondary importance for predicting the large queueing behavior. A fluid model, whose arrival process is obtained from the video data by replacing scene statistics with their means, is shown to asymptotically converge to the exact queue distribution.

Using the transition scenario of moving from one stability region to the other by a change in the value of the server capacity, we synthesize recent queueing theoretic advances and ad hoc results in video modeling, and unify a broad range of seemingly contradictory experimental observations found in the literature. As a word of caution for the widespread usage of second-order statistics modeling methods, we construct two processes with the same second-order statistics that produce distinctly different queueing behaviors.

***Index Terms*— Long-tailed distributions, MPEG, multimedia communication, multiple time scales, queueing analysis, subexponential distributions, video traffic modeling.**

I. Introduction

THE key objective of this work is to bridge the gap between video traffic *modeling* and recently developed queueing *analysis* techniques. To do this, we construct an accurate and analytically tractable model of MPEG video traffic streams. Analytically tractable models of traffic sources play a crucial part in, for example, admission control policies that ensure efficient utilization of network resources while providing quality of services guarantees. Our approach provides a unified context for explaining a number of seemingly conflicting results that have recently been reported in the literature. Along the same lines, our model applies to the full range of queueing behavior that is relevant to engineering different video applications such as real-time videoconferencing, video on demand, broadcasting, etc.

We focus on two fundamental characteristics of MPEG video streams: *multiple time scales* and *subexponentiality*. We identify the importance of these characteristics for approximate queueing analysis. Accordingly, we design a video model that accurately reflects these characteristics. The model is structured so that it is amenable to recently developed queueing theoretical analysis [1], [2].

In the literature, the existence of multiple time scale statistics in video traffic has been consistently observed by many authors. The bit rate of a video stream exhibits dependencies (correlations) that extend over a wide range of time scales, ranging from the time between consecutive cells or packets (microseconds), to consecutive frames (milliseconds), to higher level properties of video such as scenes (seconds), to entire movies or video calls.

Different modeling perspectives have been taken in examining this complex time-dependency structure. Li and Hwang, in [3], argue from the frequency domain point of view that the low frequency band of the autocorrelation's Fourier transform (long-term correlation) has the most significant impact on queueing. Lazar *et al.* [4] developed video models for the slice and frame time scales, and showed that in the case of strict quality of service (QOS) requirements (small time delay), precise modeling of the high-order autocorrelation is of secondary importance. In [5], Frost and Melamed survey a wide range of approaches to traffic modeling, several of which take multiple time scales into account, for example, self-similar or fractal models. These models essentially attempt to capture an infinite number of time scales and, for that reason, they generally suffer from high computational complexity. Landry and Stavrakakis [6] have presented a modeling approach based on multiple time scales that is appropriate for

Manuscript received May 15, 1996; revised December 31, 1996. This work was supported by the National Science Foundation under Grant CDA-90-24735. This paper was presented in part at the International IFIP–IEEE Conference on Broadband Communications, Montreal, P.Q., Canada, April 1996.

P. R. Jelenković was with the Department of Electrical Engineering, Columbia University, New York, NY 10027 USA. He is now with Bell Laboratories, Innovations for Lucent Technologies, Murray Hill, NJ 07974 USA.

A. A. Lazar and N. Semret are with the Department of Electrical Engineering and the Center for Telecommunications Research, Columbia University, New York, NY 10027 USA.

Publisher Item Identifier S 0733-8716(97)04197-8.

cell and slice levels of video traffic. The range of dependence types investigated (i.e., the shape of the autocorrelation) is restricted by the class of periodic Markov chains underlying the model.

In most of these modeling approaches, however, time scales are not explicitly represented in a manner that is suited both for queueing analysis and for computationally inexpensive traffic generation. A distinct queueing behavior that results from the multiple time scale structure of arrival processes was recently investigated in [7] and [8]. In these papers, it was analytically shown that when a stream with multiple time scales passes through a queue, the queue length distribution has multiple decay rates. Similar results were independently reported in [9]. Furthermore, a perturbation theory technique that exploits the multiple time scale structure of the arrival process and leads to a computationally efficient algorithm for evaluating the queue length distribution was developed in [8]. All of this suggests a need for video models with explicit representation of multiple time scales whose queueing behavior is analytically tractable.

The second dominant MPEG video traffic characteristic is the subexponential duration of scene lengths. Subexponential (long-range) dependence has been observed and studied in video traffic in [10], where the modeling approach was through self-similar processes. Resnick and Samorodnitsky [11] investigated the long-range dependency of the autocorrelation function of video conference traces. We observed a subexponential scene length duration in MPEG video streams (this was also seen in [12] for video coded by a simpler DPCM scheme without motion compensation), which is responsible for the long-range dependency. A calculus of almost negligable computational complexity (unlike the case of self-similar processes) for the analysis of subexponential queueing systems was recently reported in [7], [1], [13]; in those papers, it is shown that queueing systems with subexponential arrival processes exhibit queueing behavior which is very distinct from the one obtained by exploring conventional exponential models.

In this paper, we present a general model of MPEG video streams that accurately captures both the multiple time scale and subexponential characteristics of video streams.[1] The model is structured such that both of these fundamental characteristics are *explicitly represented*.

By analogy with the visual content of a video stream, i.e., its semantic structure, simple algorithms can be devised to parse the stream into a set of scenes. Subexponentiality and the slow time scale dynamics are motivated by the subexponential (Pareto) scene length duration distribution and Markovian interscene dynamics. Fast time scale dynamics are due to the independent identically distributed (i.i.d.) intrascene statistics. These statistics may vary depending on the scene. This modeling approach requires a detailed statistical analysis, and in particular evaluating the statistics of the scene lengths and their dynamics. This process may be tedious, complex, and often involves a certain amount of "eyeballing."

[1]Preliminary modeling results that concentrate only on the multiple time structure were reported in [14].

In order to alleviate this problem, we also propose a direct method for extracting some statistical parameters of the video model that exhibits a very low computational complexity and can *exactly* match any marginal distribution function and convex nonincreasing autocorrelation function (second-order statistics). We demonstrate that this method works well on real-time video data, and can be used as an alternative to the sample-path-based definitions of scenes. However, since this modeling approach is only based on second-order statistics (which do not completely determine the process), some inaccuracy in this methodology can be expected. In that regard, as a word of caution for the usage of this (or any other second-order statistics-based) method, we construct two processes that have exactly the same marginals and autocorrelation functions, but produce distinctly different queueing behavior.

Although the presented video model is rather simple, a direct queueing analysis does not appear to be straightforward. A significant simplification in the queueing analysis can be obtained, however, thanks to the structured representation of the dominant video characteristics. When a stream generated by our model is fed into a single-server queue, depending on the capacity of the queue and the buffer sizes of interest, the relative importance of the different aspects of the arrival process emerges. We identify two canonical queueing dynamics: strict and weak stability. In each of these, the relevant parts of the model are significantly simpler than in the original model, and as mentioned above, are amenable for recently developed theoretical analysis.

When *strict stability* conditions are satisfied, i.e., the conditional mean of each scene is smaller than the capacity of the server, the dominant effect in queue buildup is due to the variations on the fast time scale within each scene. In this case, a precise modeling of the interscene dynamics (long time dependency) is not essential for the accurate prediction of small to moderate queue sizes. The queue length distribution is determined using quasistationary (perturbation theory) analysis.

When *weak stability* conditions are satisfied, i.e., the conditional mean of at least one scene type is greater than the capacity of the server, the dominant effect in building a large queue size is the subexponential (long-tailed) scene length distribution. In this case, a precise modeling of intrascene statistics is of secondary importance for predicting the large queueing behavior. A fluid model, obtained from the video data by replacing scene statistics with their means, is shown to asymptotically converge to the exact queue distribution.

The results described above—namely, that in the weak stability scenario, the dominant effect on the asymptotic queueing behavior is the subexponential (long-range) dependency, and that in the strict stability scenario, the dominant effect is due to the fast time scale buildups—put in the broader context some conflicting results from the literature. Indeed, a number of authors [3], [15], [16] contend that long-range dependence of one form or another has a dominant impact on the queue, while others claim that it does not [17], [18], [4]. Our framework allows one to synthesize these results

in that the former can be viewed as instances of the weak stability scenario, while the latter are instances of the strict stability scenario. The capacity of the server that characterizes the transition from one stability scenario to the other plays a key role in understanding the queueing behavior of MPEG video streams.

This paper is organized as follows. In the next section, we present our multiple time scale model of video streams. The formal model is given in Section II-C, and the two fundamental approaches to parameter matching are detailed in Sections II-B and II-D. In Sections III and IV, we look at two typical scenarios which illustrate the impact of time scales and subexponentiality on the queueing behavior. Section V concludes the paper.

II. Modeling MPEG Video Streams

A. MPEG Video Data

The video data employed consisted of video sequences of MPEG-I frame sizes, created at the Institute of Computer Science, University of Würzburg, and are described in [19]. In all, 17 sequences (sportscasts, movies, music videos, newscasts, talk shows, cartoons, and "set top") of 40 000 frames each were available.

Taking as input the raw video frames, the MPEG coder produced three types of frames at its output.

- I frames: Only information of the current frame is used to encode it, i.e., only spatial redundancies are exploited.
- P frames: Motion compensation with respect to the previous I frame is used to achieve further compression.
- B frames: Both the previous and the next I or P frames are used to eliminate temporal redundancies, as well as spatial ones.

On average, P frames are approximately, twice the size of B frames, and one third the size of I frames. The frame types occur in a fixed periodic pattern. In this data set, the period is 12 frames, and the pattern is $IBBPBBPBBPBB$. Such a segment of 12 frames is called a group of pictures (GOP).

In this paper, we focus on the analysis and modeling of video traces on the GOP level. Thus, our basic unit or sample is the size of a GOP, i.e., the sum of the sizes of the 12 frames. Our working data set will be a sequence of 59 292 samples, formed by the concatenation of the 17 movies end to end.[2]

B. Sample Path Modeling

The basic concept which we use in separating time scales is that of scenes. As mentioned above, in this work, the unit of our video streams is the MPEG GOP, so the duration of one GOP (i.e., 12 frames, or half a second) is the basic time unit. For the behavior at the smaller time scale of a single frame, the reader is referred to [14].

[2]Note that since 40 000 is not divisible by 12, the concatenation perturbs the IPB pattern, but since we are summing over GOP's, at worst, this only affects 16 out of the 59 292 samples.

The next time scale is associated with the dynamic behavior over dozens of GOP's. By analogy with the visual content of the video stream, we call the units of this time scale *scenes*. The scenes we refer to here are defined by significant changes in the GOP size sequence, and although it makes intuitive sense to think so, it is not necessarily the case that these correspond to visual scenes.[3]

Following [12], we define a scene change to occur at a point where the normalized second difference of GOP sizes is large and negative. More precisely, let $\{\hat{A}_t : t = 1, 2, \cdots\}$ be the empirical sequence of GOP sizes. GOP t is the last of a scene if

$$\frac{[(\hat{A}_{t+1} - \hat{A}_t) - (\hat{A}_t - \hat{A}_{t-1})]}{\frac{1}{25}\sum_{j=t-24}^{t} \hat{A}_j} < -0.5. \tag{1}$$

This mechanism for extracting scenes, as well as the values of the normalization window (25 GOP's) and the threshold (-0.5), were selected empirically from a variety of methods. Among the other methods we considered is the approach of [4], which identifies scene changes as jumps $|\hat{A}_t - \hat{A}_{t-1}| > \Delta_{\min}$, subject to a minimum scene length $L_{\min}$. Indeed, there is no single "natural" definition of scenes that arises directly from the time series $\hat{A}_t$.

Fig. 1 illustrates the scene extraction from the actual MPEG GOP sequence via (1). Our full MPEG sequence of 59 292 GOP's yields 3162 scenes of mean length 18.75. Scenes constitute the basic unit at the slower time scale.

MPEG sequences can be thought of as consisting of scenes or states of a slower process, modulating the fast time scale process. For tractability purposes, however, the number of scenes is too large. Thus, our next objective is to cluster (aggregate) the scenes extracted from an MPEG video sequence into a small number of *regimes*.

In order to do so, we first characterize the scenes by the simplest possible criterion: average GOP size during the scene. Fig. 2 shows the histogram of this quantity. The scenes are classified into four types: $S, M, L,$ and XL. S and M consist of, respectively, the bottom third and middle third of the scenes (on the horizontal axis), each of the clusters having 1054 scenes. Because of the "long tail" of the histogram, we divided the top third into the two clusters L and XL, with the 856 smallest scenes in the first and the other 198 scenes in the second. More sophisticated approaches to clustering scenes have been investigated in the literature (see, for example, [20]), but we find that they do not add fundamental insights to the main conclusions of this paper.

Regime instances are formed by merging consecutive scenes of the same type. The average GOP sizes for the regimes are

$$(\lambda_S, \lambda_M, \lambda_L, \lambda_{XL}) = (1.1626, 2.1919, 3.4041, 5.9237) \times 10^5.$$

The horizontal lines in Fig. 1 show the extracted sequence of regimes. In this way, the full MPEG GOP sequence yields a

[3]Our work is based on traces of frame sizes from real video streams, but not on the actual images.

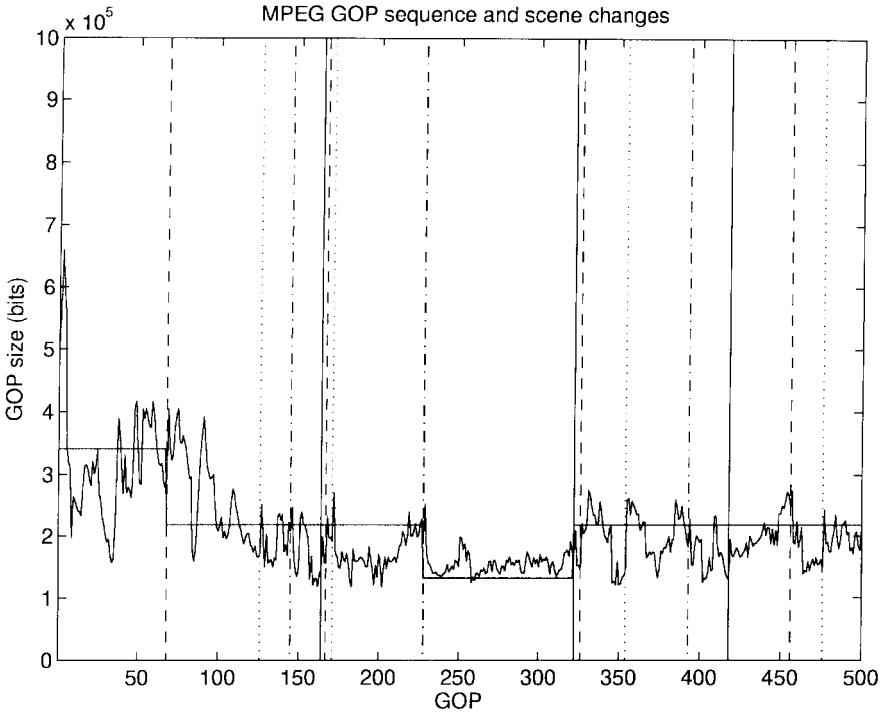

Fig. 1. Scene changes (vertical lines) and regimes (horizontal segments) in the MPEG GOP video sequence.

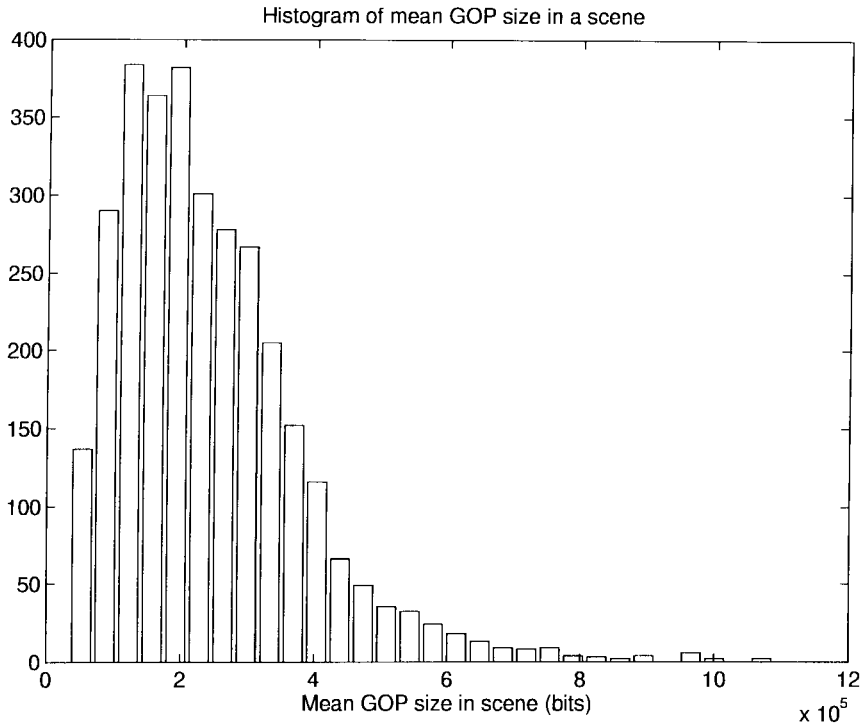

Fig. 2. Histogram of the average GOP size/scene.

sequence of 1213 regimes of the four types. The durations of regimes have the probability density functions (pdf's) shown in Fig. 3. Note that, since instances of XL regimes, by definition, occur very rarely, our data set is insufficient to obtain a meaningful distribution of duration for the XL regime. However, in constructing our model in Section II-C, based on the closeness of the duration distributions of the other three regimes, we will argue that all regimes can be modeled as having the same duration statistics. This will be further justified in Section IV, where we show that, for our purposes, the importance of the regime duration is mainly in the subexponential nature of the tail of the regime duration distribution, where the three regimes (and, we assume, the fourth) are even more similar.

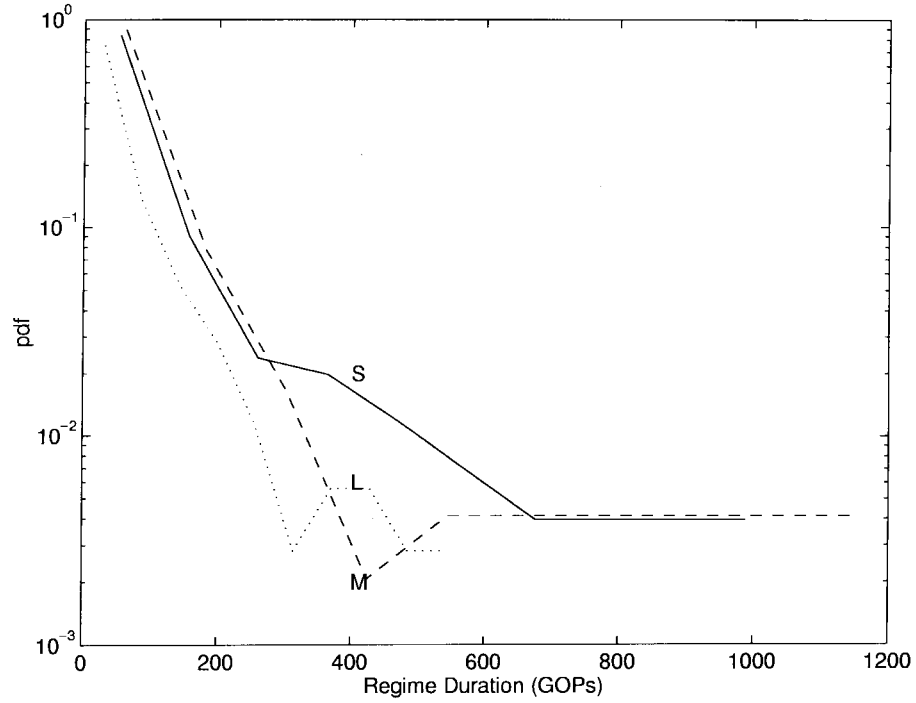

Fig. 3. Regime duration statistics.

Finally, by counting the relative frequencies of regime transitions on the sample path, we obtain the matrix of transition probabilities between regimes

$$P = \begin{pmatrix} 0 & p_{S,M} & p_{S,L} & p_{S,XL} \\ p_{M,S} & 0 & \cdots & \\ \vdots & & & \end{pmatrix} = \begin{pmatrix} 0 & 0.862 & 0.134 & 3.95e-03 \\ 0.449 & 0 & 0.501 & 4.95e-02 \\ 8.43e-02 & 0.654 & 0 & 0.261 \\ 3.39e-02 & 0.288 & 0.678 & 0 \end{pmatrix}.$$

C. A Mathematical Model for MPEG Video Streams

Let $T = \{T_0, T_1, \cdots\}$ be a sequence of renewal times, i.e., the sequence $S_n = T_n - T_{n-1} \geq 1$ is i.i.d. with a marginal distribution $F(\tau) = \mathbb{P}[S_n \leq \tau]$. The process T represents the time instances at which the video stream changes from one regime to another. Further, let $J = \{J_n, n \geq 0\}$ be a Markov chain with state space $\{S, M, L, XL\}$, and a probability transition matrix $P = (p_{ij})$, with $p_{ii} = 0$. This chain models the transitions between different regimes.

Let $B = \{B_t, t \geq 0\}$ be a process taking values in $\{S, M, L, XL\}$ and $B_t \stackrel{\text{def}}{=} J_n, T_{n-1} < t \leq T_n, n \geq 1$. B represents the indicator of the regime in which a video stream is at time t. The regime indicator process has Markovian jumps to the next state, but arbitrarily distributed sojourn times in each state. Thus, the regime indicator process B is a Markov renewal process (see, for example, [21]).

To finish the construction of the model, we define four mutually independent i.i.d. processes $X(i) = \{X_t(i), t \geq 0\}$, with marginal distribution G_i, mean λ_i, each $X(i)$ being independent of T and $J, i \in \{S, M, L, XL\}$. Each process $X(i)$ models the fast time scale statistics (intrascene "noise") for the regime i. Finally, we model the video stream as a process of the form $A = \{A_t = X_t(B_t), t \geq 0\}$, where the process of regimes B constitutes the slow time scale component that is modulated by the fast time scale "noise" process X.

Remarks: 1) The fast time scale process $X_t(i)$ could be made dependent, but as shown by the results of the following sections, the additional complexity is not necessary to obtain models that are accurate enough. This is because the time dependence is, to a large extent, accounted for by the modulating process B_t (specifically by the regime durations). 2) The sojourn times can be made state dependent, i.e., S_n, which takes values in $\{1, 2, \cdots\}$, could have distribution F_i for $J_n = i$, but this also seems unnecessary in view of Fig. 3 which shows that the different regimes types have similar duration distributions. Thus, we set $F_i = F$ for all i.

The marginals G_i of the fast time scale processes are obtained directly from the MPEG GOP traces, specifically from the histogram of the subsequence corresponding to the portions where the extracted regime is i. Thus, the (stationary) overall marginal distribution $G(x) = \mathbb{P}[A_t \leq x]$ of the model matches that of the data exactly. The sojourn time distribution F is obtained from the regime duration histograms extracted from the MPEG GOP trace (shown in Fig. 3—see Section IV for details on scene durations).

D. Second-Order Statistics-Based Modeling

A common approach to modeling video streams is to generate a stochastic process that matches its first- and second-order statistics, i.e., its marginal distribution and autocorrelation functions (ACF's) (see, for example, [22], [3], [4], [23]). For these methods to work well, it is desirable to have an easily computable expression of the ACF for the generated process

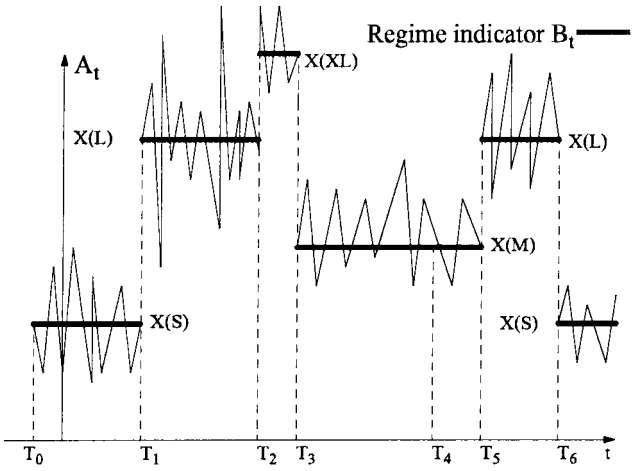

Fig. 4. Multiple time scale model of MPEG video.

in terms of model parameters. For the model presented in Section II-C above, we obtain such expressions after some further simplifying assumptions, and show how a simple model matches video traffic arbitrarily well up to second-order statistics. We present it here as an alternative to the sample path domain extraction of parameters employed in Section II-B.

Let $\pi_i \stackrel{\text{def}}{=} \mathbb{P}[B_t = i]$ denote the steady-state probability of being in regime i. Assuming that the Markov chain J is i.i.d., the ACF $R_{AA}(R_{AA}) \stackrel{\text{def}}{=} (\mathbb{E}A_0A_\tau - (\mathbb{E}A_0)^2)/\sigma^2(A_0)$ of the process $A = \{A_t, t \geq 0\}$ is given as follows.[4]

Theorem 1: If, in the model of Section II-C, the Markov chain J consists of a sequence of i.i.d. random variables and the renewal distribution is arbitrary, then ($R_{AA}(0) = 1$)

$$R_{AA}(\tau) = \frac{\sum_i \pi_i(\mathbb{E}X(i))^2 - (\mathbb{E}A_0)^2}{\sum_i \pi_i(\mathbb{E}X^2(i)) - (\mathbb{E}A_0)^2}\,[1-F_1(\tau)] \qquad \tau \geq 1$$

where $F_1(\tau) \stackrel{\text{def}}{=} 1/m\sum_0^\tau [1-F(u)]$, $m \stackrel{\text{def}}{=} \mathbb{E}S_n$ is the residual distribution for the renewal distribution F.

Proof: Follows from straightforward algebra. ◇

Remark: A simple asymptotic expresion for the ACF is also available when J is Markovian and the renewal times are subexponential (see Appendix B for the definition of subexponential distributions). This result (Theorem 4) is presented in Section IV together with the other results on subexponential distributions.

The expression above gives us substantial flexibility in adjusting model parameters to fit an empirical ACF. In all other known models, however, there is no *explicit* expression for estimating model parameters for exactly matching a given ACF. This is usually done by heuristic searches in the parameter space. Here, we can overcome this substantial obstacle, at the expense of further simplifying the model, by assuming that the noise processes are constant, i.e., $X(i) \equiv \lambda_i$. Thus, A reduces to a simple fluid model, with constant rate arrivals in each renewal interval that are chosen independently from previous intervals (regime indicator lines in Fig. 4 illustrate the sample path of the fluid model). We call this type of process a *space–time renewal process* (SRP); the name comes from the fact that both space and time are renewal. The expression in the above theorem now becomes

$$R_{AA}(\tau) = 1 - m^{-1}\sum_0^\tau [1 - F(u)]. \tag{2}$$

The ACF is exactly equal to the integrated tail of the renewal distribution function. Therefore, given an ACF R_{AA}, it is easy to obtain the regime duration distribution F.

From (2), by setting $\tau = 1$ ($F(0) = 0$), we get

$$m = \frac{1}{1 - R_{AA}(1)} \tag{3}$$

and $[1-R_{AA}(\tau+1)] - [1-R_{AA}(\tau)] = m^{-1}[1-F(\tau)]$ yields

$$F(\tau) = 1 - m[R_{AA}(\tau) - R_{AA}(\tau+1)]. \tag{4}$$

For F to be a probability distribution, it must be nondecreasing, which implies that R_{AA} must be *convex*, and $F \leq 1$ implies that R_{AA} must be *nonincreasing*. Finally, consistency calls for $m = \sum_{\tau=0}^\infty [1 - F(\tau)] = \sum_{\tau=0}^\infty m[R_{AA}(\tau) - R_{AA}(\tau+1)]$. Since $R_{AA}(0) = 1$, this implies that we must have $\lim_{\tau\to\infty} R_{AA}(\tau) = 0$.

Strengths of the SRP Approach: The main strengths of this modeling approach are the following. First, it provides an arbitrarily exact match of the first- and second-order statistics, a property which is not achieved by any other known method. Second, a very broad and realistic class of AFC's can be matched, including, for example, Markovian models such as the Markov-modulated Poisson process of Skelly *et al.* [17], the TES-based models [22], or the DAR models [24]. Note that all of these examples taken from the literature can only match exponentially decreasing ACF's. Third, an SRP model can match *subexponential* ACF's, and as such, it is a uniquely efficient and simple model capturing long-range dependence. Note that the $M/G/\infty$ arrival model (see [16]) also displays great flexibility in modeling second-order statistics with subexponential autocorrelation structure. We refer the reader to [16, Proposition 4.2] for the explicit form of the ACF of the $M/G/\infty$ arrival process. However, there is no explicit algorithm to extract $M/G/\infty$ model parameters from the second-order statistics of an empirical trace. (Precise fluid queue asymptotics with $M/G/\infty$ arrivals were obtained in [13], [2], and [25].) Fourth, in the presence of long-tailed renewal times, Theorem 2 (see Section IV-B) further justifies the usage of the fluid type models.

We now use this SRP model to generate traffic matching that of 17 MPEG sources multiplexed (summed) into one stream. For clarity, we consider the stream at the GOP level, where the measured ACF exhibits the desired (convex, decreasing) properties. Fig. 5 shows portions of sample paths for the real and generated traffic, and how well the statistics match.[5]

In conclusion, independent of whether one uses a sample path (as in Section II-B) or a statistics-based approach (as in the this section) for obtaining the parameters of the regime

[4] For the general case of a non i.i.d. modulating chain, we give asymptotic relations in Section IV.

[5] That, however, is not the end of the story—see Appendix A.

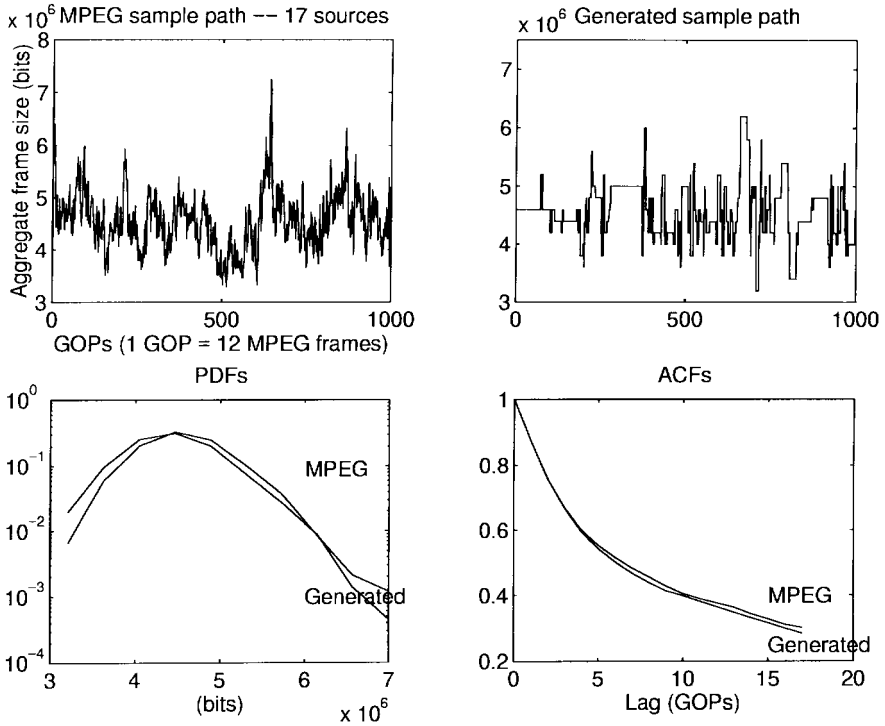

Fig. 5. Matching first- and second-order characteristics of MPEG video.

duration distribution F, the main strength of the general model presented in Section II-C is that it provides a single framework in which to view the different characteristics which are relevant to traffic engineering for the full range of video communications services. This is further demonstrated in Sections III and IV.

III. Strictly Stable Queue: Fast Time Scale Build-Ups

Consider a single-server queue with the arrival process A_t and constant server capacity C, whose queue size Q_t at time t is defined by Lindley's recursion

$$Q_t = (Q_{t-1} - C + A_t)^+. \tag{5}$$

For the rest of the paper, we assume that Q_t is the unique stationary solution to the recursion (5) (see [26]), i.e., we assume that the queue is in its steady state. The arrival process $A = (A_t), t \geq 0$, represents the mathematical model for MPEG video streams as described in Section II-C.

In this section, we consider the case of what we call a *strictly stable* queue. This is the case when the capacity of the server is greater than the mean arrival rate in the "worst case" regime λ_{XL}. Fig. 6 illustrates this case.

The queue will build up only when the arrivals exceed the server capacity (the value indicated by the horizontal line). Under the strict stability condition, this tends to happen with occasional large peaks (see Fig. 6), and not with sustained bursts since the capacity is above the mean rate of even the worst regime (the regimes and their mean GOP sizes are shown by the horizontal segments). Thus, it is more important to capture these peaks (which are in the fast time scale process) rather than the slow time scale bursts (i.e., the duration of regimes).

Under the strictly stable condition, the queueing behavior is approximately given by the following superposition result (see the superposition theorem in [7] and [8]):

$$\mathbb{P}[Q_t = x] \approx \sum_{i \in \{S,M,L,XL\}} \pi_i \Pr[Q_t(i) = x] \tag{6}$$

where $Q_t(i)$ is the queue size obtained by feeding the queue only with regime i, and π_i is the steady-state probability of being in regime i. Informally, this result should be understood as $\mathbb{P}[Q_t = x] / \sum_{i \in \{S,M,L,XL\}} \pi_i \mathbb{P}[Q_t(i) = x] \to 1$ as the holding times of the regimes approach ∞. In the formal proof of this result, which can be found in [8], the limit is taken only with respect to the regime sojourn times, and the buffer size x is kept fixed (finite). Therefore, this result gives good approximations when the average renewal (regime duration) times are much larger than the time unit (one GOP) and the buffer sizes are small to moderately large. A refinement of (6) based on perturbation theory asymptotic expansion series can be found in [8].

Fig. 7 shows the queue length pdf's resulting from queueing simulations of the type defined by (5) for five different sequences. In the top plot, the queue is fed by each of the four subsequences of the empirical GOP trace corresponding to the regime types. The bottom plot of Fig. 7 compares the weighted sum of the four queue distributions with the queue distribution for the full empirical sequence (GOP trace). The server capacity $C = \lambda_{XL}/0.9$ satisfies the strict stability condition. The close match between the superposition of the four regimes and the full sequence verifies (6).

This suggests that *the fast time scale i.i.d. processes are sufficient for capturing the queueing behavior due to the different regimes*. To corroborate this, Fig. 8 compares the queue

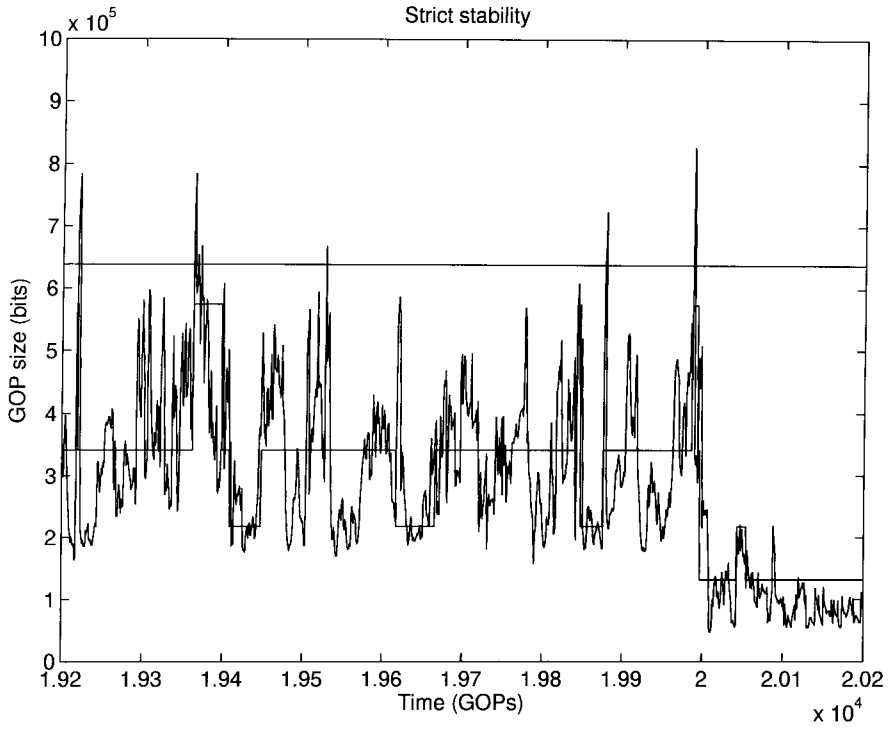

Fig. 6. MPEG GOP trace; the horizontal line shows the server capacity satisfying strict stability.

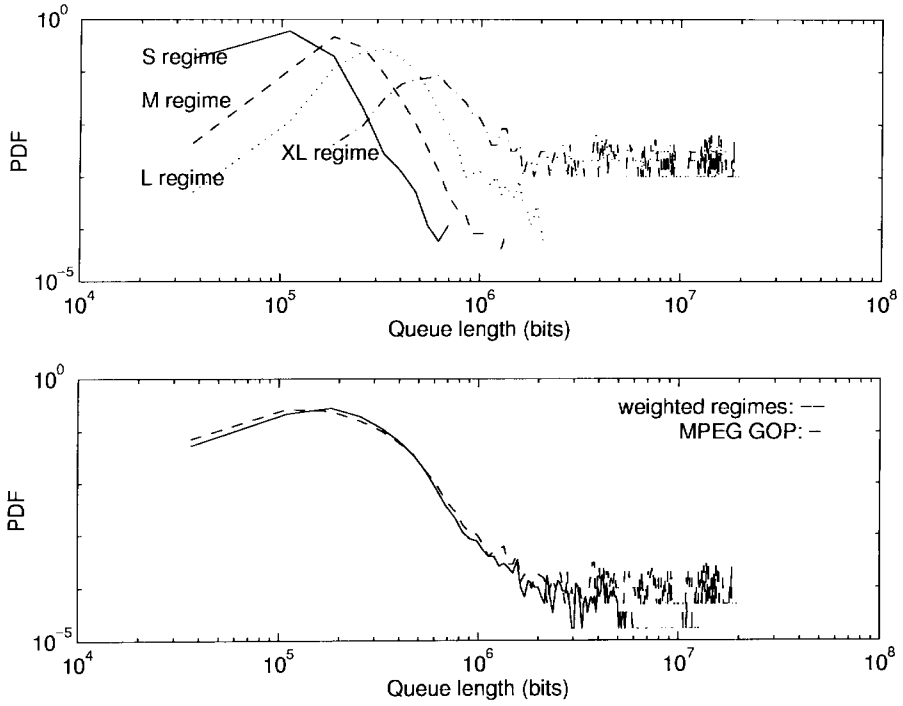

Fig. 7. Under strict stability, MPEG GOP satisfies superposition principle; see text for details.

length distributions obtained when the traffic is generated by two instances of the model we described in Section II-C, with the queue length distribution resulting from the actual MPEG GOP trace. The first instance of the model has a Pareto regime duration distribution F, and the second has a geometric distribution. In both cases, the mean equals the mean regime duration of the empirical MPEG GOP trace. The closeness of the queue length distributions (at least for the small buffer sizes) for the two model instances supports the claim that (6) holds in the strict stability scenario: the slow time scale dynamics do not come into play since knowledge of the steady-state regime probabilities π_i is enough. Thus, the specific form of the dependency structure (here, Pareto or geometric) is of little consequence.

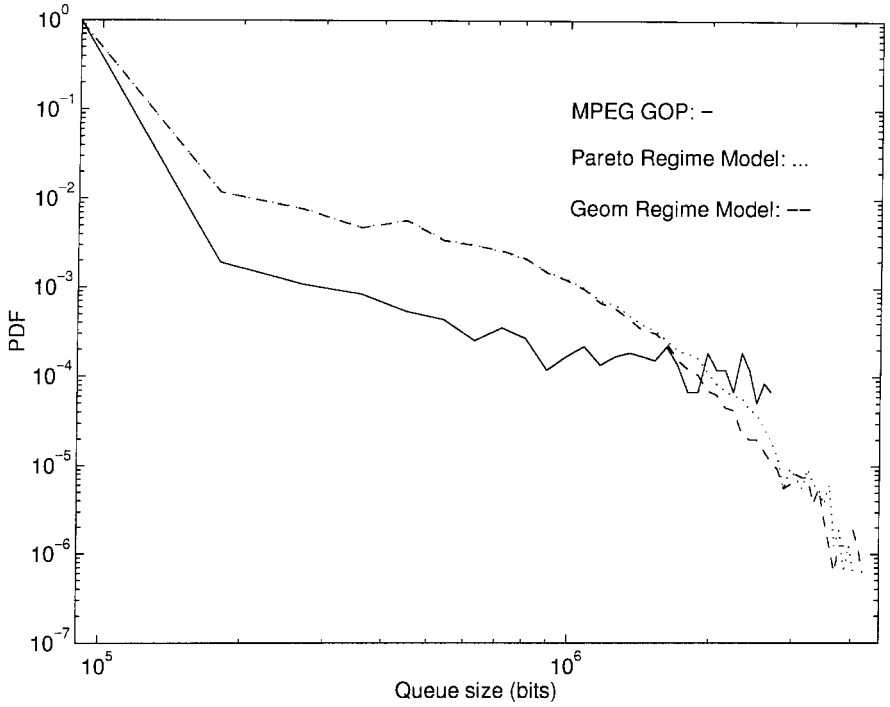

Fig. 8. Strictly stable queue pdf for MPEG GOP and generated model.

The relatively low computational complexity of (6) justifies our multiple time scale approach to modeling, at least in the strict stability case: if strict stability is the realistic context (i.e., if the maximum buffer size and cell loss requirements are stringent), then one can concentrate the modeling effort, separately, on each of the regimes. *The multiple time scale nature of the traffic needs to be taken into account up to the mean regime durations*. Higher order statistics of the slow time scale variations do not offer significant additional improvements (for small buffer sizes).

Thus, for the purpose of analytical predictions of queueing behavior, one computes the queue length distribution associated with each of the simple processes $X_t(i)$, and weights them by π_i. For the purpose of traffic generation, the advantage is that one need not expend too much effort in estimating the parameters of F as long as the mean is accurate; this is especially useful with heavy-tailed regime durations (i.e., long-range dependency) whose parameters are difficult to estimate.[6]

Often, for the purpose of a network admission controller seeking to guarantee a given quality of service while efficiently utilizing resources, one wants to accurately estimate the tail of the queue, and derive from that the traffic stream's "equivalent bandwidth" [27]. However, a simple-minded application of the notion of equivalent bandwidth based only the decay rate of the queue tail would, in this case, overestimate the queue by a factor of $1/\pi_{XL}$ (i.e., two orders of magnitude), and thus result in an underutilization of resources. This is because the asymptotic decay rate of the queue distribution depends mainly on the "worst case" regime XL. Indeed, for queue lengths of 10^6 bits or more, the contribution of that regime to the summation in (6) is at least ten times that of any of the three other regimes (see Fig. 7). This is in line with [28, Th. 2].

The above observations for the strict stability scenario help in the understanding of recent work by a number of authors. Skelly *et al.* [17] observed that, although the "presence of strong correlation is important for capturing the queueing behavior of video, the actual form of the correlation is not." Ryu and Elwalid [18] argued that for "realistic ATM traffic engineering," "long term correlations do not have significant impact on the cell loss rate." Similarly, Lazar *et al.* [4] observed that precise modeling of long-term correlation is of secondary importance for "real-time" scheduling. These observations are in full agreement with our modeling approach to MPEG video streams, and can be readily explained in the context of the strict stability scenario that we described in this section.

In the following section, we show that when the queue is weakly stable, the form of the dependency plays a dominant role in the associated queueing behavior, especially for large buffer sizes, and particularly when this dependency (the regime durations) is subexponential in nature, as is the case for MPEG video streams.

IV. Weakly Stable Queue: Subexponential Bursts

A. Queueing Behavior

In the second scenario, the queue is *weakly stable*, meaning that the capacity, although still above the overall mean of the arrival stream, may be below the mean of one or more "unstable" regimes. This may not be the appropriate context for real-time interactive services, i.e., video streams with small delay bounds. However, for services such as video on

[6] Note that, since the total length of the data set (the MPEG GOP sequence) is 59 292, the points at "probabilities" below 10^{-4} are statistically meaningless for the queue distribution of the MPEG GOP trace.

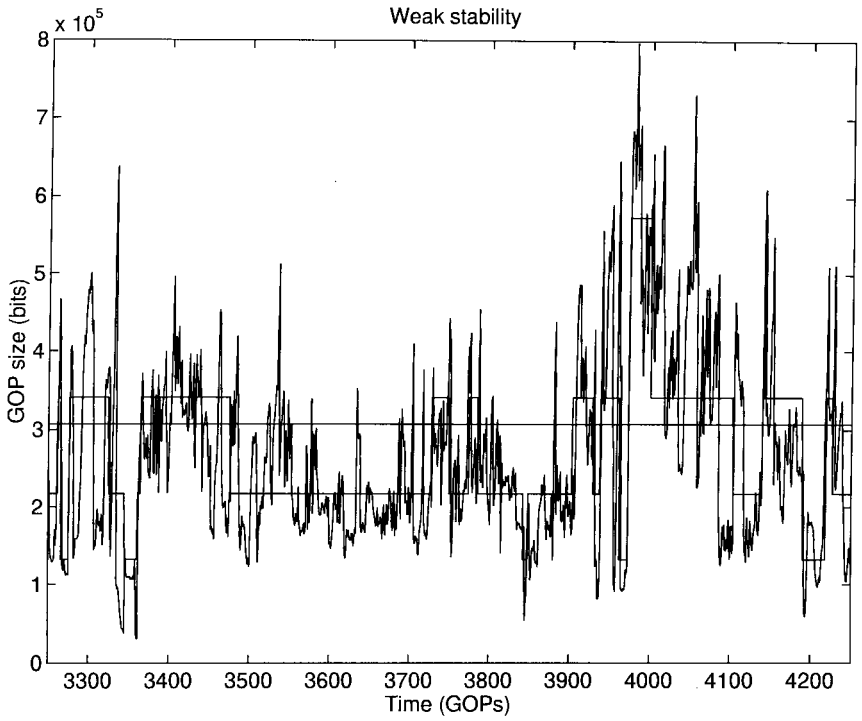

Fig. 9. Weak stability: the horizontal line shows the server capacity.

demand (VOD) or broadcasting, understanding the behavior in a scenario with large buffers and tolerance for long delays may be important. In this section, we show how the same model can be used for modeling and analyzing this end of the spectrum of video communication services.

Fig. 9 illustrates the weak stability case. Here, the queue tends to be built up by sustained bursts (i.e., by the unstable regimes) that require service beyond the capacity of the server. The duration of the regimes is then critical for the queue length distribution.

The density of durations for all four types of regimes combined is shown in Fig. 10. A Pareto function of the form (β/τ^{α}) gives an accurate match (a Pareto function was also found to match scene durations of VBR video in [12]). If the density of the durations was exponentially decaying, as it would be in a purely Markov-modulated model, it would appear as a straight line on the log-scaled plot. Thus, MPEG traffic exhibits *subexponential* behavior on the slow time scale. Some basic definitions and results on long-tailed and subexponential distributions are given in Appendix B.

The demonstrated subexponentiality of scene lengths plays a crucial role in the queueing behavior in the weak stability scenario. Consider the case of the server having a capacity of $C = \lambda_L$. Out of the four regimes, XL is unstable and L is marginally stable; the queue is stable with respect to the overall arrival stream.

Simulations were performed with the MPEG GOP stream and two model-generated streams, respectively. The first generated stream has Pareto-distributed regime durations, where the Pareto function is identical to the one shown in Fig. 10. The second has geometrically distributed regime durations. In all three streams, the regime durations have *the same mean*.

Two generated sample paths *of regime durations* are illustrated in Fig. 11. The top, which has the Pareto marginal, clearly exhibits the subexponential characteristic of having large isolated peaks, unlike the geometric sequence, which has an exponentially decaying pdf.

Remark: Intuitively, if $X_1, X_2, \cdots, X_n$ are independent, identically, and subexponentially distributed random variables

$$\mathbb{P}[X_1 + X_2 + \cdots + X_n > x] \sim n\mathbb{P}[X_1 > x] \qquad (7)$$

as $x \to \infty$. This means that a sum of subexponential random variables exceeds a large value x by having one of them exceed this value. In other words, in the i.i.d. sequence, the biggest peaks tend to be isolated, and since subexponential distributions are "heavy tailed," roughly speaking, these biggest peaks are extremely large and dominate the sequence.

Fig. 12 shows the resulting queue length distributions under weak stability. The figure shows that the Pareto-distributed regime duration captures the salient features of the queue length distribution, which the geometric regime duration does not. Note that by the superposition result described in Section III, under *strict* stability conditions, since they have the same mean regime durations, all three would have the same queue distribution.

Thus, the dominant effect on the queueing behavior is the subexponential regime duration. The fast time scale has little impact in the weak stability scenario. To verify this, we also simulated the queue with the SRP "fluid flow" version of our model. Recall that the SRP model is simply the special case that is obtained by removing the fast time scale "noise," i.e., setting $X(i) \equiv \lambda_i$. The fourth curve in Fig. 12 (for the fluid model with Pareto regime durations) shows that it is indeed true that the fast time scale does not affect the asymptotic

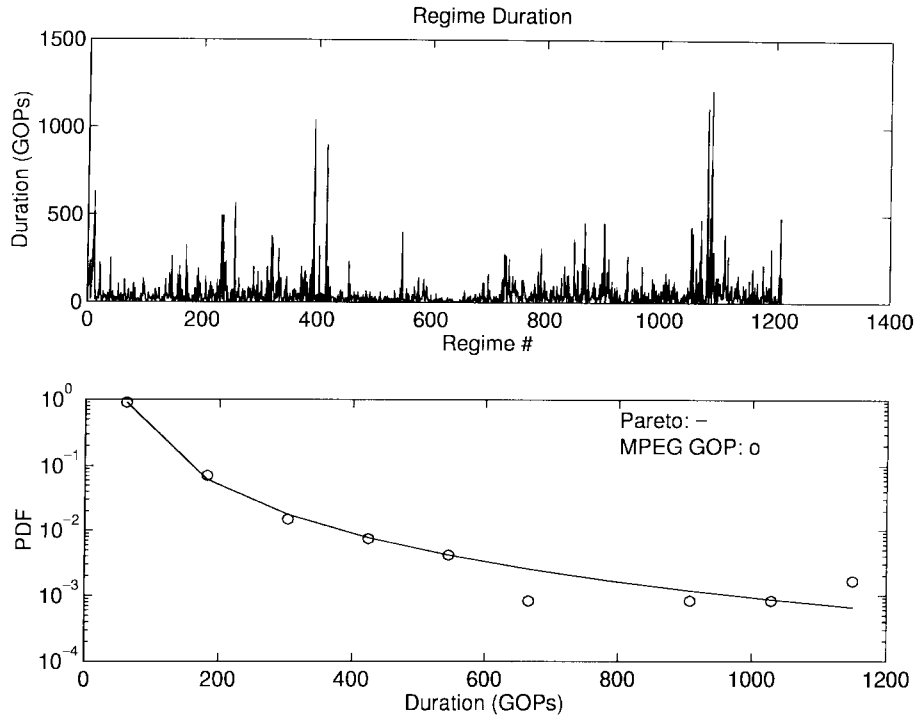

Fig. 10. MPEG GOP regime durations (top), and duration density compared to Pareto $(2.68 \times 10^4/t^{2.47})$ (bottom).

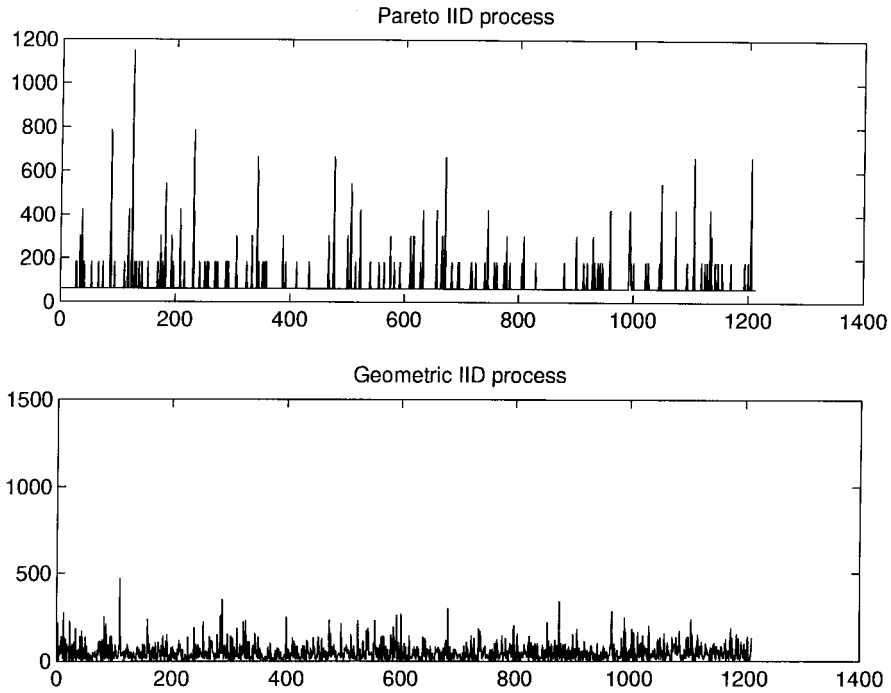

Fig. 11. Sample paths of subexponentially (top) and exponentially (bottom) distributed processes with the *same mean.*

queueing behavior. The same figure also suggests that the SRP model might accurately predict the tail behavior of the queue for large buffer sizes. This observation will be made precise in the following section.

The key feature that we will be investigating in the rest of this paper is the queue tail. This tail can be attributed to the subexponentiality of the regime durations of the arrival process. Indeed, the queue tail density corresponding to an arrival stream with geometric (exponentially decaying) scene durations has a constant slope on the log scale which is steeper than the tail corresponding to an arrival stream with Pareto regimes. Thus, for very large buffers (for the example of the simulation, a buffer size greater of 10^8 bits or more), a Markovian model with exponentially decaying (geometric) regime durations would severely underestimate delays and loss probabilities. This is clearly apparent in Fig. 13, where

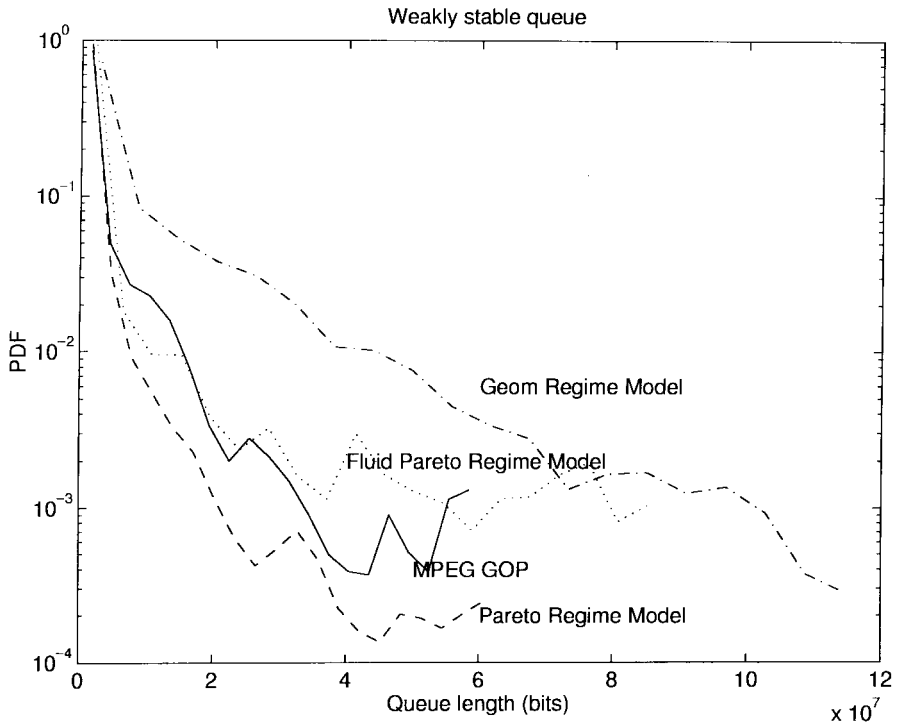

Fig. 12. Weakly stable queue length pdf for MPEG GOP trace and models with subexponential (Pareto) and exponential (geometric) scene durations.

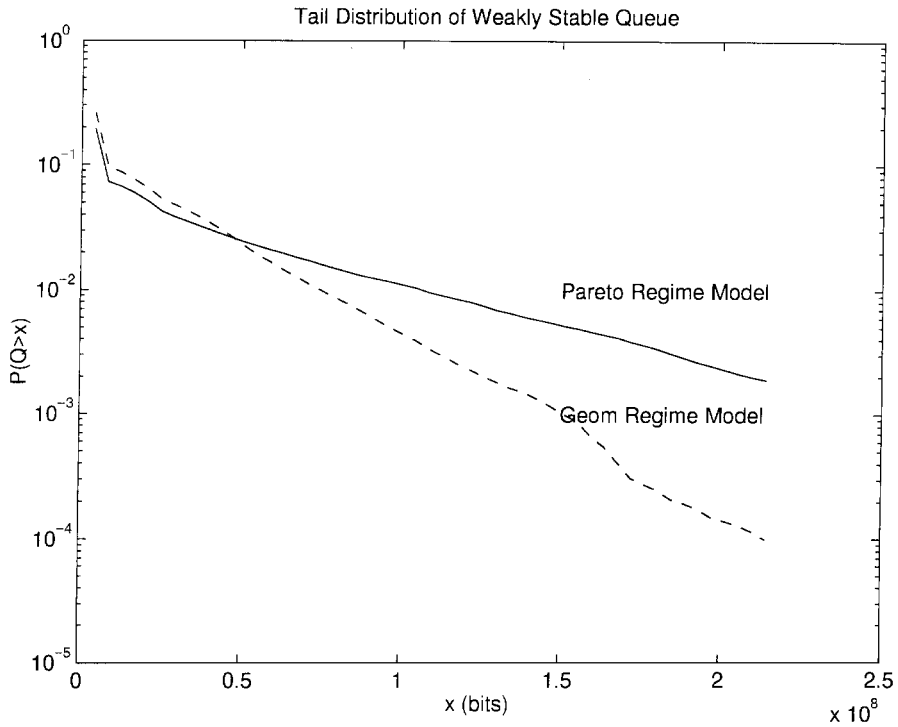

Fig. 13. Exponential regime durations underestimate large buffer probabilities.

the integrated tail $P(Q > x)$—which closely approximates buffer overflow probabilities—of the queue generated by the two models is shown. At small buffer sizes, the Markovian model overestimates the buffer size. This is because, in order to have the same mean as the subexponential (heavy-tailed) distribution, the geometric distribution has to have a bulkier midsection, i.e., regimes of medium size happen more often. Thus, compared to the MPEG stream and the Pareto model, the geometric model generates more regimes of "medium" duration, and thus has more often a queue of medium length, but would have fewer of the very long regimes which make the queue build up to very large sizes.

Due to the limited amount of data, we cannot draw more than qualitative conclusions purely from the MPEG trace-

driven simulations. This is even more so for the subexponential asymptotics since the processes converge to their steady state only with subexponential speed (see [1]). However, we are able to infer the dominant queueing behavior for our model with subexponential regime durations. That in itself is a valuable lesson for simulation studies of video traffic behavior: "it takes a very long time" to obtain accurate results on subexponential statistics. Thus, it is all the more important to have the analytical tools to calculate the queue distribution.

B. A Fluid Model and Queueing Asymptotics

The simulations indicate that, under weak stability, the tail of the queue length pdf is subexponential (respectively, exponential) when the slow time scale statistics are subexponential (respectively, exponential). As we shall presently show, analysis confirms this observation. Our modeling approach leads directly to an analytical estimation of the tail of the queue length distribution.

First, the asymptotic accuracy of the SRP fluid model is presented in Theorem 2. Second, an elegant and computationally efficient queueing formula for the fluid model is obtained in Theorem 3. Third, we investigate the ACF of our video model in Theorem 4, and some of its simplifications in Corollary 1. Fourth, Theorem 5 directly relates the queueing and the ACF asymptotic behavior. A summary of the intersection of all these results is given in Corollary 2. All of the results in the rest of this section apply both in the continuous- and discrete-time case. For the continuous-time versions, the corresponding sums should be replaced by integrals.

Recall that the arrival stream is of the form $A_t = X_t(B_t)$, where B_t is a Markov renewal process with arbitrarily distributed durations, and given i, $X_t(i)$ is an i.i.d. sequence with mean λ_i. Now consider the process obtained by sampling the queue length at the renewal epochs: $Q_n \equiv Q_{T_n}$. Contrary to the strictly stable case where precise modeling of the scene length distribution was of secondary importance, in the weakly stable case, the regime duration distribution plays the dominant role for large buffer occupancy probabilities. The following theorem illustrates this point precisely.

Consider the fluid version of the model in which the $X(i)$'s are replaced by the means $\lambda_i = \mathbb{E}X(i)$, and denote the arrival process by A_t^f. Let us denote by Q_n^f the queue length process, corresponding to the fluid approximation arrivals (A^f) sampled at the renewal times. Further, assume that, in the full model, the "noise" processes $X_t(i)$ satisfy the following Cramér conditions.

Cramér Conditions: There is a positive constant θ such that $\mathbb{E}e^{\theta X_t(i)} < \infty$ for all i.

Recall that, for both queueing processes, we assume that Q_n and Q_n^f are in their unique stationary regimes (see [26]).

Theorem 2: Assume that the renewal distribution $F \in \mathcal{R}_\alpha$ (distributions of regular variation defined in Appendix B; the Pareto family β/x^α is in $\mathcal{R}_\alpha$), and that the *Cramér conditions* are satisfied. Then, assuming that the queue is weakly stable

$$\lim_{x\to\infty} \frac{\mathbb{P}[Q_n > x]}{\mathbb{P}[Q_n^f > x]} = 1.$$

Proof: Given in Appendix C.

Remarks: 1) This result strongly supports the fluid models (see [29]) that have much lower computational complexity; 2) related asymptotic results in the Markovian framework that justify the fluid approximation were obtained in [9] and [30]; 3) this result can be proved under the weaker assumption that the distribution of the renewal times is intermediately regularly varying [13]. Due to the space constraints and the need for introducing new definitions, we avoid stating this result in its most general form.

Intuitively, the result of Theorem 2 can be explained as follows. In the subexponential world, large queue build-ups happen in an isolated fashion. When the queue is weakly stable, a large excursion of the process Q_n basically results from one long isolated regime during which the average arrival rate exceeds the server capacity. Assume that when this overflow happens, the arrival process is in regime i. Then, the total server overflow during this long renewal period S_n is approximately $\sum_{t=T_n}^{T_{n+1}}[X_t(i) - C] \approx S_n[\mathbb{E}X_t(i) - C]$; to make this approximation rigorous is the technical difficulty involved in proving Theorem 2.

A simple illustration of the preceding theorem is given with the following simulation example. Assume that the modulating chain J_n is a two-state valued Bernoulli process with $\mathbb{P}[J_n = 1] = 1 - \mathbb{P}[J_n = 0] = p = 0.4$; when in state 0, there are no arrivals (i.e., $X_t(0) \equiv 0$,) and when in state 1, the conditional arrivals $X_t(1)$ are Bernoulli with $\mathbb{P}[X_t(1) = 0] = \mathbb{P}[X_t(1) = 4] = 1/2$. The renewal distribution is assumed to be Pareto with $\mathbb{P}[S_n \geq t] = 1/t^3, t = 1, 2, 3, \cdots$. The corresponding fluid model is the one in which the "noise" process $X_t(1)$ is replaced by its mean $\mathbb{E}X_t(1) = 2$. Simulation results are presented in Fig. 14 (for a sample path length of 2×10^9.)

The fluid model is much easier to analyze. The queue length sampled at the renewal times $Q_n^f \equiv Q_{T_n}^f$ satisfies the following recursion:

$$Q_{n+1}^f = [Q_n^f + S_n(A_{T_n}^f - C)]^+ \tag{8}$$

(recall that $S_n \stackrel{\text{def}}{=} T_{n+1} - T_n$). Then, the asymptotic tail behavior of the queue length distribution is given by the following result.

Let $x_i \stackrel{\text{def}}{=} \lambda_i - C$. Recall that $\mathcal{S}$ is the class of subexponential distributions (defined in Appendix B), and similarly to the defintion of F_1, let H_1 be the residual distribution of H, i.e., $H_1(t) \stackrel{\text{def}}{=} 1/m \sum_{u=0}^{t}[1 - H(u)]$, $m \stackrel{\text{def}}{=} \mathbb{E}\sum_{u=0}^{\infty}[1 - H(u)]$, and $\bar{H}(t) \stackrel{\text{def}}{=} 1 - H(t)$.

Theorem 3: Let the stability condition $\mathbb{E}A_t^f < C$ be satisfied, and suppose that for all $x_i > 0$, there is a distribution H such that $H, H_1 \in \mathcal{S}$, and $\mathbb{P}[S_n > t/x_i]/\bar{H}(t) \to w_i$, as $t \to \infty$, with at least one $w_i > 0$. Then

$$\mathbb{P}[Q_n^f > x] \sim \frac{1}{\mathbb{E}S_n(C - \mathbb{E}A_t)} \sum_{u=x}^{\infty} \mathbb{P}[S_n(\lambda_{B_n} - C) > u]$$

as $x \to \infty$.

Proof: Follows from [1, Th. 6]. ◇

The following theorem establishes the direct asymptotic relation between the renewal time distribution function and the ACF.

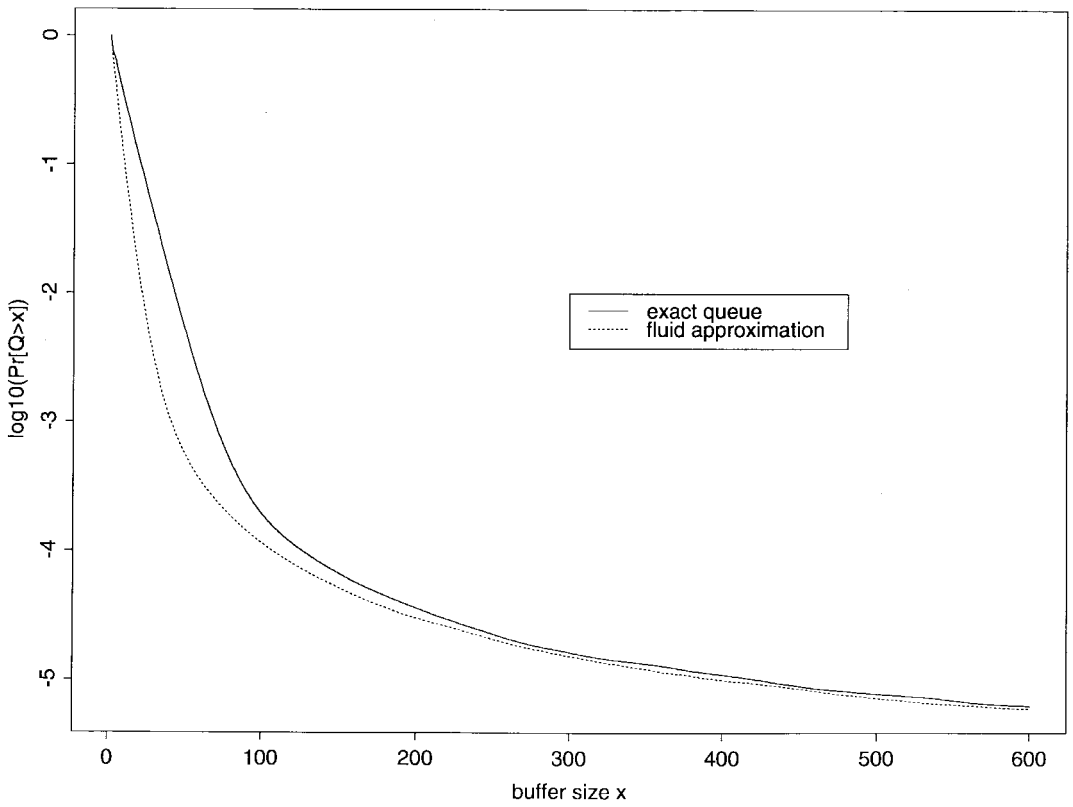

Fig. 14. Comparison between the fluid approximation and the actual queue length distribution.

Theorem 4: Assume that the renewal distribution function is subexponential. Then, the autocorrelation function R_{AA} satisfies the following asymptotic relation:

$$R_{AA}(\tau) \sim \frac{\sum_i \pi_i(\mathbb{E}X(i))^2 - (\mathbb{E}A_0)^2}{\sum_i \pi_i(\mathbb{E}X(i)^2) - (\mathbb{E}A_0)^2}[1 - F_1(\tau)]$$

where $\pi_i = \mathbb{P}[B_t = i]$, and $F_1(\tau) \stackrel{\text{def}}{=} 1/m \sum_{u=0}^{\tau} [1 - F(u)]$, $m \stackrel{\text{def}}{=} \mathbb{E}S_n$ is the residual distribution for the renewal distribution F.

Proof: Exactly the same proof as for [1, Th. 7] applies here. ◇

Intuitively speaking, the relatively simple and elegant structure of the autocorrelation asymptotics in the previous theorem is because the asymptotics induced by the subexponential regime holding times eventually wins over the exponential (Markovian) dependency introduced by the Markovian jumps, and therefore the Markovian dependency is not visible in the asymptotic domain. There are several corollaries of this theorem. The following corollary is [1, Th. 7].[7]

Corollary 1: The ACF of the fluid arrival model A_t^f is given by

$$R_{AA}^f(\tau) \sim [1 - F_1(\tau)].$$

Proof: Follows from Theorem 4. ◇

[7]Theorem 1 is another corollary for the special case when the Markovian jumps are replaced by independent state transitions. Then, instead of the asymptotic relation, we get equality.

Now, if in Theorem 3 the distribution H can be chosen to be equal to F (renewal distribution) $H \equiv F$, then by combining Theorem 3 and Corollary 1, we establish the asymptotic proportionality of the ACF function with the queue length distribution.

Theorem 5: If, in Theorem 3, the distribution H can be chosen to be $H \equiv F$, then

$$\mathbb{P}[Q_n^f > \tau] \sim r R_{AA}^f(\tau), \qquad \tau \to \infty$$

for an appropriately chosen positive constant r.

Proof: [1, Th. 8]. ◇

Remarks: 1) If the distribution function of S_n belongs to the regularly varying functions (Pareto family), the assumption $\mathbb{P}[S_n > t/x_i] \sim w_i \bar{F}(t), w_i > 0$, will be satisfied for all $x_i > 0$, i.e., we can choose $H \equiv F$. 2) This is the first result that rigorously relates the arrival process ACF and the queue length distribution. It also explains why, in the recent literature, much attention has been given to investigating the impact of the ACF on the queueing behavior [3], [31], [4].

The constant in the previous theorem can be explicitly calculated if the renewal distribution F is assumed to be a regularly varying distribution $F \in \mathcal{R}_\alpha$. Recall from the definition of regular variation (see Appendix B) that $F \in \mathcal{R}_\alpha$ has an explicit representation of the form $1 - F(\tau) \sim l(\tau)/\tau^\alpha$ as $\tau \to \infty$, where $l(\tau)$ is a slowly varying function (see again Appendix B).

Corollary 2: If $F \in \mathcal{R}_\alpha$, and if the queue is weakly stable, then

$$\begin{aligned}\mathbb{P}[Q_n > \tau] &\sim \mathbb{P}[Q_n^f > \tau] \\ &\sim \frac{\sum_{x_i>0} \pi_i x_i^\alpha}{\mathbb{E}S_n(C-\mathbb{E}A_t)} \sum_{u=\tau}^{\infty} \mathbb{P}[S_n > u] \\ &\sim \frac{\sum_{x_i>0} \pi_i x_i^\alpha}{\mathbb{E}S_n(C-\mathbb{E}A_t)} \frac{l(\tau)}{(\alpha-1)\tau^{\alpha-1}} \\ &\sim \frac{\sum_{x_i>0} \pi_i x_i^\alpha}{\mathbb{E}S_n(C-\mathbb{E}A_t)} \\ &\quad \cdot \frac{\sum_i \pi_i(\mathbb{E}X^2(i)) - (\mathbb{E}A_0)^2}{\sum_i \pi_i(\mathbb{E}X(i))^2 - (\mathbb{E}A_0)^2} R_{AA}(\tau) \\ &\sim \frac{\sum_{x_i>0} \pi_i x_i^\alpha}{\mathbb{E}S_n(C-\mathbb{E}A_t)} R_{AA}^f(\tau)\end{aligned}$$

as $\tau \to \infty$; recall that $x_i \stackrel{\text{def}}{=} \lambda_i - C$, and R_{AA}^f represents the ACF of the fluid model.

Proof: The first asymptotic relation is just Theorem 2. The second and the third follow from Theorem 3, and

$$\begin{aligned}\sum_{u=\tau}^{\infty} \mathbb{P}[S_n(\lambda_{J_n} - C) > u] &\sim \sum_{x_i>0} \pi_i \sum_{u=\tau}^{\infty} \frac{l(u/x_i)}{(u/x_i)^\alpha} \\ &\sim \sum_{x_i>0} x_i^\alpha \pi_i \frac{l(\tau)}{(\alpha-1)\tau^{\alpha-1}} \\ &\sim \sum_{x_i>0} x_i^\alpha \pi_i \sum_{u=\tau}^{\infty} \mathbb{P}[S_n > u]\end{aligned}$$

as $\tau \to \infty$. The fourth and the fifth statements of the theorem follow by straightforward combination of the second asymptotic relation and Theorem 4 and Corollary 1, respectively.

◇

V. Conclusion

We have shown that real-time MPEG video traffic exhibits both multiple time scale and subexponential characteristics, and have presented a video traffic model that captures both of these characteristics. MPEG sequences were modeled as consisting of scenes or states of a slower process modulating fast time scale processes. To make the model more tractable, scenes extracted from the MPEG video sequence were aggregated into a small number of regimes. Subexponentiality (long tails) was observed to characterize the regime length distribution. We showed that model parameters can be obtained by using sample path and second-order statistics-based approaches. The model provided a framework for studying MPEG video traffic in two representative operating scenarios called weakly stable and strictly stable.

It should be noted that our modeling approach could be applied to faster time scales, e.g., on the slice/frame or even cell/slice time scale. Provided the subexponentiality and multiple time scale nature of the corresponding quantities is preserved, the same analysis will apply. We will consider this in our future work, where we will also elaborate on the important issue of multiplexing video streams with subexponential statistics [13].

Appendix A
A Word of Caution on Second-Order Statistics-Based Models

While the universality of the statistics-based approaches appears attractive in comparison with the somewhat arbitrary choice made in the time domain extraction of video features such as scenes, one should note that there is a danger in matching first- and second-order statistics blindly. As will be shown shortly, it is possible to achieve a perfect match of those statistics and still completely fail to capture the queueing behavior.

It is clear that a process is just partially defined by its ACF and marginal distribution function (second-order statistics). Therefore, there might be many different processes which have these two statistics the same, and a natural question to ask is: How different can the queue be when these processes are fed into it? As we shall see in this section, the queueing behavior can be very different. Along the same lines, for the domain of self-similar processes, in [16] it was shown that the Hurst parameter alone is inadequate for characterizing the long-range dependency.

Example 1: Let us take $C = 1$, and construct the following Bernoulli-type renewal arrival process A_t. Take a stationary renewal process $\{T_n, n \geq 0\}$ with renewal distribution F; and take two Bernoulli processes with the distribution $\mathbb{P}[X_t(i) = 2] = 1 - \mathbb{P}[X_t(i) = 0] = b_i, i = 1, 2$. Further, at the beginning of each renewal interval, we flip a coin with a probability of success p; if the success occurs, then in the current interval (say $[T_n, T_{n+1})$), we define $A_t = X_t(1)$, and $A_t = X_t(2)$ otherwise.

Now, it is easy to compute the marginal distribution of the arrival process A_t

$$\mathbb{P}[A_t = 2] = 1 - \mathbb{P}[A_t = 0] = pb_1 + (1-p)b_2.$$

From Theorem 1, we compute the ACF for this process

$$\begin{aligned}R_{AA}(\tau) = &\frac{(pb_1^2 + (1-p)b_2^2) - (pb_1 + (1-p)b_2)^2}{(pb_1 + (1-p)b_2) - (pb_1 + (1-p)b_2)^2} \\ &\cdot (1 - F_1(\tau)).\end{aligned}$$

From the two equations above, we can see that the two processes characterized by the triples $(p_i, b_{1,i}, b_{2,i}, i = 1, 2)$ will have the same ACF and m.d.f. as long as the following set of equations is satisfied:

$$p_1 b_{1,1} + (1-p_1)b_{2,1} = p_2 b_{1,2} + (1-p_2)b_{2,2} \quad (9)$$

$$p_1 b_{1,1}^2 + (1-p_1)b_{2,1}^2 = p_2 b_{1,2}^2 + (1-p_2)b_{2,2}^2. \quad (10)$$

Consider now a numerical example of two processes [that satisfy (9)] characterized by $(p_1 = 0.4, b_{1,1} = 0.4, b_{2,1} = 0)$, and $(p_2 = 0.1, b_{1,2} = 0.747878, b_{2,2} = 0.09468)$, and

a renewal distribution $\mathbb{P}[T_n - T_{n-1} \geq t] = 1/t^{1.6}, t = 1, 2, \cdots$. It is evident that the queue fed with the first arrival process is strictly stable, while the queue fed with the second arrival process is not. Therefore, for the stable case, we have that the queue length asymptotics is exponential since it is stochastically smaller than the queue for which the arrival process is Bernoulli with $\mathbb{P}[A_t = 2] = 0.4$. On the other hand, in the second case, due to weak stability, Corollary 2 implies that the queue is going to be asymptotically proportional to the integrated tail of the renewal distribution (which is long tailed) and, therefore, it will display a polynomial decay. The simulated ACF is represented on the top part of Fig. 15 (the minor differences between the ACF's come from the finiteness of the simulated sample paths). The respective queue length distributions are given at the bottom part of the same figure; the solid line represents the first exponentially decaying queue, and the dotted line represents the second polynomially decaying queue.

Appendix B
Some Theoretical Results on Subexponential Distributions

Definition 1: A distribution function F on $[0, \infty)$ is called *long tailed* ($F \in \mathcal{L}$) if

$$\lim_{x \to \infty} \frac{1 - F(x - y)}{1 - F(x)} = 1, \qquad y \in \mathbb{R}. \tag{11}$$

Definition 2: A distribution function F on $[0, \infty)$ is called *subexponential* ($F \in \mathcal{S}$) if

$$\lim_{x \to \infty} \frac{1 - F^{*2}(x)}{1 - F(x)} = 2 \tag{12}$$

where F^{*2} denotes the second convolution of F with itself, i.e., $F^{*2}(x) = \int_{[0,\infty)} F(x - y)F(dy)$.

The class of subexponential distributions was first introduced by Chistakov [32]. Some examples of distribution functions in $\mathcal{S}$ are the following.

1) Distributions of regular variations $\mathcal{R}_\alpha$ (contains Pareto distributions)
$$F(x) = 1 - \frac{l(x)}{x^\alpha}$$
$\alpha > 0$, and $l(x)$ being a slowly varying function, i.e., $\lim_{x \to \infty} l(\delta x)/l(x) = 1$ for all $\delta > 0$ (this class of distributions was first introduced in [33]).
2) The lognormal distribution
$$F(x) = \Phi\left(\frac{\log x - \mu}{\sigma}\right), \qquad \mu \in \mathbb{R}, \sigma > 0$$
where Φ is the standard normal distribution.
3) Weibull distribution
$$F(x) = 1 - e^{-x^\beta}$$
for $0 < \beta < 1$.
4)
$$F(x) = e^{-x(\log x)^{-a}}$$
for $a > 0$.
5) Benktander Type I distribution [34]
$$F(x) = 1 - cx^{-a-1}x^{-b \log x}(a + 2b \log x)$$
$a > 0, b > 0$, and c appropriately chosen.
6) Benktander Type II distribution [34]:
$$F(x) = 1 - cax^{-(1-b)} \exp\{-(a/b)x^b\}$$
$a > 0, 0 < b < 1$, and c appropriately chosen.

In what follows, we will state two basic results on subexponential distributions. The general relation between $\mathcal{S}$ and $\mathcal{L}$ is the following.

Lemma 1: (Athrey and Ney [35]) $\mathcal{S} \subset \mathcal{L}$.

Lemma 2: If $F \in \mathcal{L}$, then $(1 - F(x))e^{\alpha x} \to \infty$ as $x \to \infty$, for all $\alpha > 0$.

Note: Lemma 2 clearly shows that for long-tailed distributions, Cramér-type conditions are not satisfied.

Appendix C
Weak Stability: Proof of Theorem 2

In this section, we provide the proof of Theorem 2. Observe first that the queue length observed at the renewal times satisfies the following queue length recursion:

$$Q_{T_{n+1}} = \max(Q_{T_n} + Z_{T_{n+1}}, Y_{T_{n+1}}) \tag{13}$$

where

$$Z_{T_{n+1}} \stackrel{\text{def}}{=} \sum_{i=T_n+1}^{T_{n+1}} (A_i - C)$$

and

$$Y_{T_{n+1}} \stackrel{\text{def}}{=} [\max_{T_n < k \leq T_{n+1}} \sum_{i=k}^{T_{n+1}} (A_i - C)]^+$$

. (Recall that, for simplicity reasons, since the queue length is only observed at the renewal times, we denoted $Q_{n+1} \equiv Q_{T_{n+1}}$.)

Lower Bound: First we will prove that $\liminf_{x \to \infty} \mathbb{P}[Q_n > x]/\mathbb{P}[Q_n^f > x] \geq 1$. Since $Y_{T_{n+1}} \geq 0$, we have

$$\begin{aligned} Q_{T_{n+1}} &\geq M_{n+1} \\ &\stackrel{\text{def}}{=} \sup(Z_{T_{n+1}}, Z_{T_{n+1}} + Z_{T_n}, Z_{T_{n+1}} + Z_{T_n} + Z_{T_{n-1}}, \cdots). \end{aligned}$$

From the inequality above, we see that the lower bound will follow if we manage to prove that $\lim_{x \to \infty} \mathbb{P}[M_n > x]/\mathbb{P}[Q_n^f > x] = 1$. The last equality will follow from [1, Th. 6], if we prove that the conditional increments in the random walk M_n and in the fluid queueing process Q_n^f have the same asymptotics. More precisely, we need to prove the following lemma.

Lemma 3:

$$\lim_{x \to \infty} \frac{\mathbb{P}[Z_{T_n} > x | J_n = i]}{\mathbb{P}[S_n > x]} = \lim_{x \to \infty} \frac{\mathbb{P}[S_n(\lambda_i - C) > x]}{\mathbb{P}[S_n > x]} \tag{14}$$

where

$$\lambda_i \stackrel{\text{def}}{=} \mathbb{E}[A_t | T_n \leq t < T_{n+1}, J_n = i],$$

and

$$S_n \stackrel{\text{def}}{=} T_{n+1} - T_n.$$

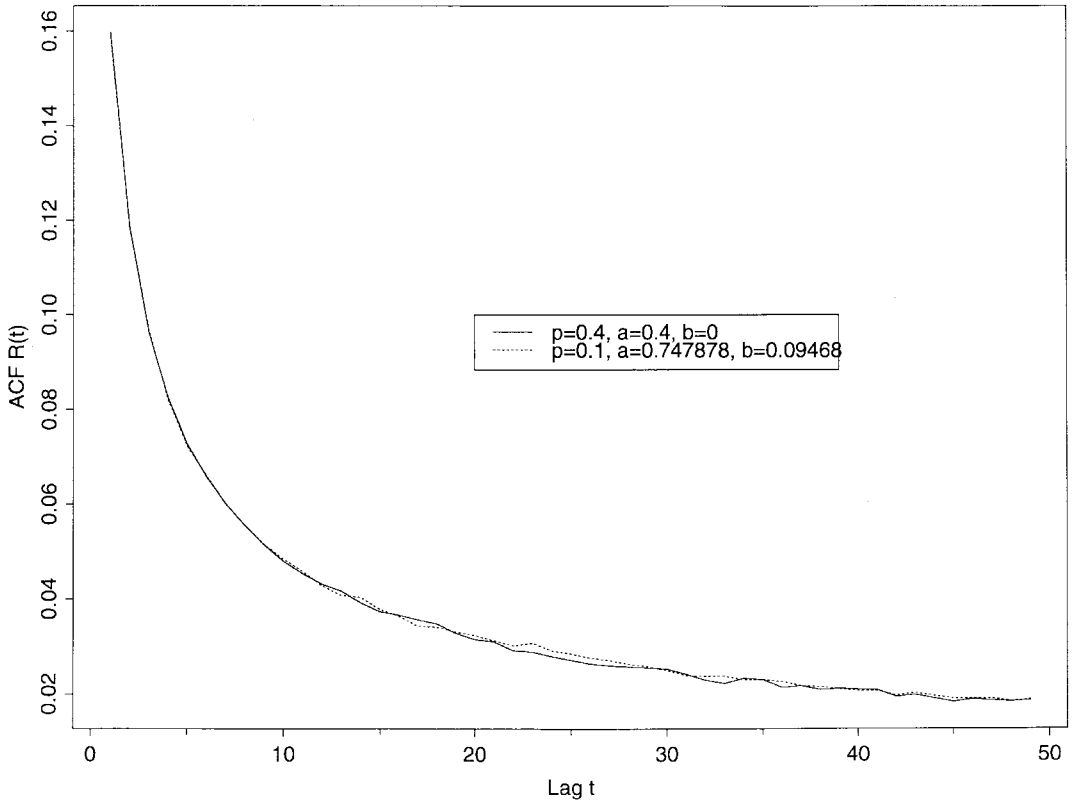

(a)

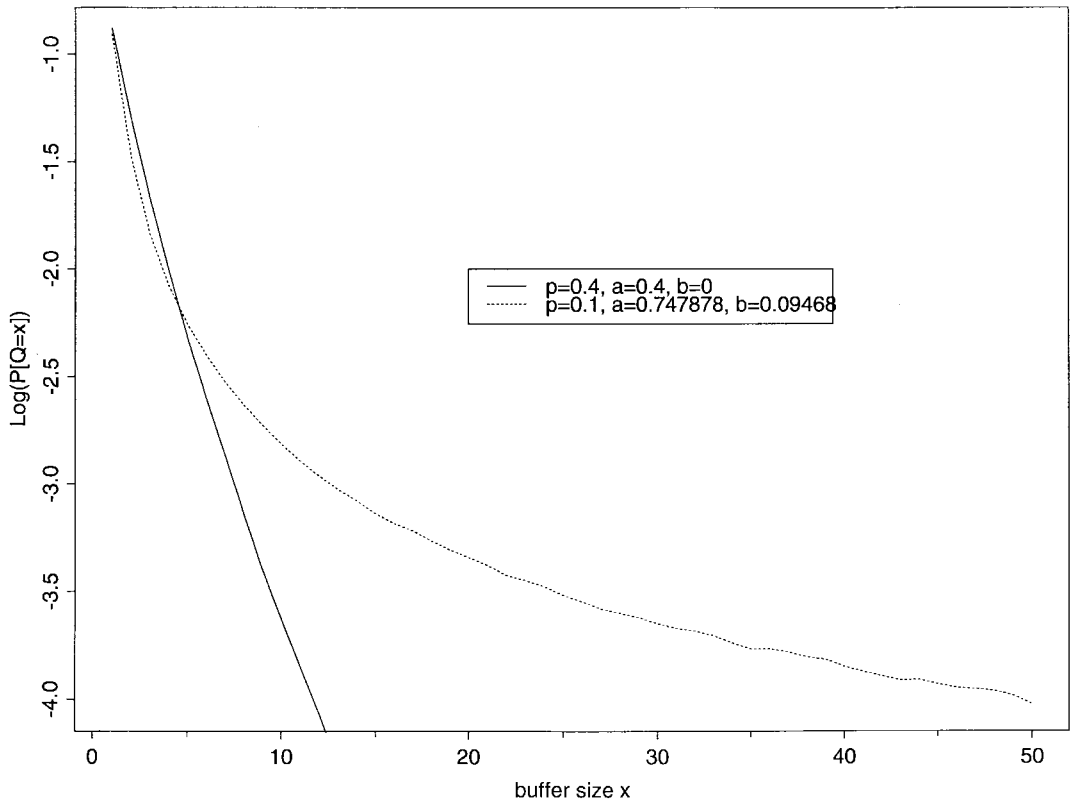

(b)

Fig. 15. Two processes with the same marginal d.f. and the same ACF's (a) that build very different queues (b).

Proof: If $\lambda_i < C$, then the right-hand side of (14) is equal to zero. The left-hand side will be equal to zero if we show that $\mathbb{P}[Z_{T_n} > x | J_n = i]$ decays exponentially in x, and that will follow from

$$\mathbb{P}[Z_{T_n} > x | J_n = i] \le \sum_{k=1}^{\infty} \mathbb{P}\left[\sum_{t=1}^{k} (X_t(i) - C) > x\right] \le de^{-\delta x}$$

for some constants $d, \delta > 0$. The latter inequality follows from the Cramér conditions imposed on $X_t(i)$.

If $\lambda_i > C$, then

$$\begin{aligned}
&\mathbb{P}[Z_{T_n} > x | J_n = i] \\
&\quad = \sum_{k=1}^{\infty} \mathbb{P}[S_n = k] \mathbb{P}\left[\sum_{t=1}^{k} (X_t(i) - C) > x\right] \\
&\quad \le \sum_{k=1}^{\lfloor x/\lambda_i - C + \epsilon \rfloor} \mathbb{P}[S_n = k] \mathbb{P}\left[\sum_{t=1}^{k} (X_t(i) - C) > x\right] \\
&\qquad + \mathbb{P}\left[S_n > \frac{x}{\lambda_i - C + \epsilon}\right] \qquad (15)
\end{aligned}$$

where $\lfloor y \rfloor$ denotes the integer part of y. Again, from the Cramér conditions, it follows that the sum in (15) decays exponentially for any $\epsilon > 0$. Therefore, for any $\epsilon > 0$

$$\begin{aligned}
&\limsup_{x\to\infty} \frac{\mathbb{P}[Z_{T_n} > x | J_n = i]}{\mathbb{P}[S_n > x]} \\
&\quad \le \limsup_{x\to\infty} \frac{\mathbb{P}\left[S_n > \dfrac{x}{\lambda_i - C + \epsilon}\right]}{\mathbb{P}[S_n > x]} \\
&\quad = \left(\frac{\lambda_i - C + \epsilon}{\lambda_i - C}\right)^{\alpha} \lim_{x\to\infty} \frac{\mathbb{P}[S_n(\lambda_i - C) > x]}{\mathbb{P}[S_n > x]}
\end{aligned}$$

the last equality follows from $S_n \in \mathcal{R}_\alpha$. Therefore, by passing $\epsilon \to 0$, we obtain

$$\lim_{x\to\infty} \frac{\mathbb{P}[Z_{T_n} > x]}{\mathbb{P}[S_n > x]} \le \lim_{x\to\infty} \frac{\mathbb{P}[S_n(\lambda_i - C) > x]}{\mathbb{P}[S_n > x]}. \qquad (16)$$

To prove the reversed inequality, observe that

$$\begin{aligned}
&\mathbb{P}[Z_{T_n} > x | J_n = i] \\
&\quad \ge \sum_{\lfloor x/\lambda_i - C - \epsilon \rfloor}^{\infty} \mathbb{P}[S_n = k] \mathbb{P}\left[\sum_{j=1}^{k} (X_j(i) - C) > x\right] \\
&\quad \ge \mathbb{P}\left[\sum_{j=1}^{\lfloor x/\lambda_i - C - \epsilon \rfloor} (X_j(i) - C) > x\right] \\
&\qquad \cdot \mathbb{P}\left[S_n \ge \left\lfloor \frac{x}{\lambda_i - C - \epsilon} \right\rfloor\right].
\end{aligned}$$

By observing that for each $\epsilon > 0$, $\mathbb{P}[\sum_{j=1}^{\lfloor (x/\lambda_i - C - \epsilon) \rfloor} (X_j(i) - C) > x]$ converges to one exponentially fast, in the same spirit as in proving inequality (16), we prove the reversed inequality of (16). This finishes the proof of lemma, and the lower bound part of the proof of Theorem 2. ◇

Upper Bound: Here, we compare Q_n with a fluid queue $Q_n^{f,\epsilon}$ that has slightly larger arrivals than Q_n^f, i. e., we assume that the arrival process to the queue $Q_n^{f,\epsilon}$ is $A_t^{f,\epsilon} \stackrel{\text{def}}{=} A_t^f + \epsilon$, where $\epsilon > 0$ is sufficiently small so that $Q_n^{f,\epsilon}$ represents a stable queue.

By iterating recursion (13), we obtain that

$$Q_n = \sup(Y_{T_n}, Z_{T_n} + Y_{T_{n-1}}, Z_{T_n} + Z_{T_{n-1}} + Y_{T_{n-2}}, \cdots).$$

Further observe that

$$\begin{aligned}
Y_{T_n} &\le \left[\sup_{T_n < k \le T_{n+1}} \sum_{i=k}^{T_{n+1}} (A_i - A_i^{f,\epsilon})\right]^+ \\
&\qquad + \left[\sup_{T_n < k \le T_{n+1}} \sum_{i=k}^{T_{n+1}} (A_i^{f,\epsilon} - C)\right]^+ \\
&\stackrel{\text{def}}{=} \Delta Y_{T_n} + (Z_{T_n}^{f,\epsilon})^+
\end{aligned}$$

where $Z_{T_n}^{f,\epsilon} \stackrel{\text{def}}{=} \sum_{i=T_n+1}^{T_{n+1}} (A_i^{f,\epsilon} - C)$. By defining further $\Delta A_{T_n} \stackrel{\text{def}}{=} \sum_{i=T_n+1}^{T_{n+1}} (A_i - A_i^{f,\epsilon})$, we obtain that Q_n is bounded by

$$\begin{aligned}
Q_n \le \sup(&0, \Delta Y_{T_n}, \Delta A_{T_n} + \Delta Y_{T_{n-1}}, \Delta A_{T_n} \\
&+ \Delta A_{T_{n-1}} + \Delta Y_{T_{n-2}}, \cdots) \\
+ \sup(&0, Z_{T_n}^{f,\epsilon}, Z_{T_n}^{f,\epsilon} + Z_{T_{n-1}}^{f,\epsilon}, \\
&Z_{T_n}^{f,\epsilon} + Z_{T_{n-1}}^{f,\epsilon} + Z_{T_{n-2}}^{f,\epsilon}, \cdots).
\end{aligned}$$

The second $\sup(\cdot)$ in the inequality above is exactly equal to $Q_n^{f,\epsilon}$; the first $\sup(\cdot)$ we denote by S^ϵ. Then, it follows that

$$\mathbb{P}[Q_{T_n} > x] \le \mathbb{P}[Q_{T_n}^{f,\epsilon} + S^\epsilon > x].$$

From the Cramér conditions, it is relatively easy to see that for every $\epsilon > 0$, S^ϵ is an exponentially bounded random variable, i.e., there exist $d, \delta > 0$, such that $\mathbb{P}[S^\epsilon > x] \le de^{-\delta x}$. Therefore, it follows:

$$\begin{aligned}
\mathbb{P}[S^\epsilon + Q_{T_n}^{f,\epsilon} > x] &= \mathbb{P}[S^\epsilon + Q_{T_n}^{f,\epsilon} > x, S^\epsilon < \sqrt{x}\,] \\
&\quad + \mathbb{P}[S^\epsilon + Q_{T_n}^{f,\epsilon} > x, S^\epsilon \ge \sqrt{x}\,] \\
&\le \mathbb{P}[Q_{T_n}^{f,\epsilon} > x - \sqrt{x}\,] + \mathbb{P}[S^\epsilon \ge \sqrt{x}\,] \\
&\le \mathbb{P}[Q_{T_n}^{f,\epsilon} > x - \sqrt{x}\,] + de^{-\delta\sqrt{x}}.
\end{aligned}$$

Since from [1, Th. 6], it follows that $\mathbb{P}[Q_{T_n}^{f,\epsilon} > x]$ has a

regularly varying tail, we come to the conclusion that

$$\limsup_{x\to\infty}\frac{\mathbb{P}[Q_n>x]}{\mathbb{P}[Q_n^f>x]}\le\frac{\sum_{x_i+\epsilon>0}\pi_i(x_i+\epsilon)^\alpha}{\sum_{x_i>}\pi_i x_i^\alpha}$$

for all sufficiently small $\epsilon>0$. By passing $\epsilon\to 0$, we obtain

$$\limsup_{x\to\infty}\frac{\mathbb{P}[Q_n>x]}{\mathbb{P}[Q_n^f>x]}\le 1.$$

This finishes the proof of the theorem. ◇

ACKNOWLEDGMENT

The authors would like to thank the Institute of Computer Science at the University of Würzburg for making the MPEG video traces available. They would also like to thank the anonymous reviewers for their in-depth comments on the original paper.

REFERENCES

[1] P. R. Jelenković and A. A. Lazar, "Subexponential asymptotics of a Markov-modulated random walk with queueing applications," *J. Appl. Prob.*, vol. 35, June 1998.
[2] ——, "Multiplexing on-off sources with subexponential on periods: Part II," *ITC 15*, Washington, DC, June 1997.
[3] S. Qi Li and C.-L. Hwang, "Queue response to input correlation functions: Discrete spectral analysis," *IEEE/ACM Trans. Networking*, vol. 1, pp. 317–329, Oct. 1993.
[4] A. A. Lazar, G. Pacifici, and D. E. Pendarakis, "Modeling video sources for real-time scheduling," *Multimedia Syst.*, vol. 1, no. 6, pp. 253–266, 1994.
[5] V. S. Frost and B. Melamed, "Traffic modeling for telecommunication networks," *IEEE Commun. Mag.*, pp. 70–81, Mar. 1994.
[6] R. Landry and I. Stavrakakis, "Multiplexing ATM traffic streams with time-scale-dependent arrival processes," preprint, Mar. 1995.
[7] P. R. Jelenković and A. A. Lazar, "Multiple time scale and subexponential asymptotic behavior of a network multiplexer," *Stochastic Networks: Stability and Rare Events*, P. Glasserman and K. Sigman, and D. D. Yao, Eds., Lecture Notes. Berlin, Germany: Springer-Verlag, 1996.
[8] P. R. Jelenković, "The effect of multiple time scales and subexponentiality on the behavior of a broadband network multiplexer," Ph.D. dissertation, Dep. Elect. Eng., Columbia Univ., New York, 1996.
[9] D. N. C. Tse, R. G. Gallager, and J. N. Tsitsiklis, "Statistical multiplexing of multiple time-scale Markov streams," *IEEE J. Select. Areas Commun.*, vol. 13, pp. 1028–1038, Aug. 1995.
[10] J. Beran, R. Sherman, M. S. Taqqu, and W. Willinger, "Long-range dependence in variable bit-rate video traffic," *IEEE Trans. Commun.*, vol. 43, pp. 1566–1579, 1995.
[11] S. Resnick and G. Samorodnitsky, "Performance decay in a single server exponential queueing model with long range dependence," preprint, 1996.
[12] D. P. Heyman and T. V. Lakshman, "Source models for vbr broadcast-video traffic," *IEEE/ACM Trans. Networking*, vol. 4, pp. 40–48, Feb. 1996.
[13] P. R. Jelenković and A. A. Lazar, "Multiplexing on-off sources with subexponential on periods: Part I," in *Proc. IEEE INFOCOM'97*, Kobe, Japan, Apr. 1997.
[14] P. R. Jelenković, A. A. Lazar, and N. Semret, "Multiple timescales and subexponentiality in MPEG video streams," in *Proc. Int. IFIP–IEEE Conf. Broadband Commun.*, L. Mason and A. Casaca, Eds., Montreal, Canada, Apr. 1996.
[15] N. Likhanov, B. Tsybakov, and N. D. Georganas, "Analysis of an ATM buffer with self-similar (fractal) input traffic," in *Proc. IEEE INFOCOM'95*, Boston, MA, Apr. 1995, pp. 985–991.
[16] M. Parulekar and A. M. Makowski, "Tail probabilitites for a multiplexer with self-similar traffic," in *Proc. IEEE INFOCOM'96*, San Fancisco, CA, Mar. 1996.
[17] P. Skelly, S. Dixit, and M. Schwartz, "A histogram based model for video traffic behavior in an ATM network node with an application to congestion control," in *Proc. IEEE INFOCOM'92*.
[18] B. K. Ryu and A. Elwalid, "The importance of long-range dependence of VBR video traffic in ATM traffic engineering," in *Proc. ACM SIGCOMM*, 1996.
[19] O. Rose, "Statistical properties of MPEG video traffic and their impact on traffic modeling in ATM systems," Inst. Comput. Sci., Univ. Würzburg, Tech. Rep. 101, 1995.
[20] B. Melamed and D. Pendarakis, "A Markov-renewal-modulated TES model for VBR Star Wars video," preprint.
[21] E. Cinlar, *Introduction to Stochastic Processes.* Englewood Cliffs, NJ: Prentice-Hall, 1975.
[22] B. Melamed, D. Raychaudhuri, B. Sengupta, and J. Zdepski, "TES-based traffic modeling for performance evaluation of integrated networks," in *Proc. IEEE INFOCOM'92*, May 1992.
[23] M. R. Ismail, I. Lambdaris, M. Devetsikiotis, and A. R. Kaye, "Modeling prioritized MPEG video using tes and a frame spreading strategy for transmission in ATM networks," in *Proc. IEEE INFOCOM'95*, Apr. 1995, pp. 762–769.
[24] A. Elwalid, D. Heyman, T. V. Lakshman, D. Mitra, and A. Weiss, "Fundamental bounds and approximations for ATM multiplexers with applications to video teleconferencing," *IEEE J. Select. Areas Commun.*, vol. 13, no. 6, 1995.
[25] P. R. Jelenković and A. A. Lazar, "Asymptotic results for multiplexing subexponential on-off sources," *Adv. Appl. Prob.*, July 1996.
[26] R. M. Loynes, "The stability of a queue with non-independent inter-arrival and service times," *Proc. Cambridge Phil. Soc.*, vol. 58, pp. 497–520, 1968.
[27] R. Guerin, H. Ahmadi, and M. Nagshineh, "Equivalent capacity and its application to bandwidth allocation in high-speed networks," *IEEE J. Select. Areas Commun.*, vol. 9, pp. 968–981, 1991.
[28] P. R. Jelenković and A. A. Lazar, "On the dependence of the queue tail distribution on multiple time scales of ATM multiplexers," in *Conf. Inform. Sci. Syst.*, Baltimore, MD, Mar. 1995, pp. 435–440, http://comet.ctr.columbia.edu/publications.
[29] A. I. Elwalid and D. Mitra, "Effective bandwidth of general Markovian traffic sources and admission control of high speed networks," *IEEE/ACM Trans. Networking*, vol. 1, pp. 329–343, June 1993.
[30] G. L. Choudhury, A. Mandelbaum, M. I. Reiman, and W. Whitt, "Fluid and diffusion limits for queues in slowly changing environments," preprint, 1996.
[31] M. Livny, B. Melamed, and A. K. Tsiolis, "The impact of autocorrelation on queueing systems," *Manag. Sci.*, vol. 39, pp. 322–339, 1993.
[32] V. P. Chistakov, "A theorem on sums of independent positive random variables and its application to branching random processes," *Theor. Prob. Appl.*, vol. 9, pp. 640–648, 1964.
[33] J. Karamata, "Sur un mode de croissance réguilière des fonctions," *Mathematica (Cluj)*, 1930.
[34] C. Kluppelberg, "Subexponential distributions and integrated tails," *J. Appl. Prob.*, vol. 25, pp. 132–141, 1988.
[35] K. B. Athreya and P. E. Ney, *Branching Processes*. Berlin, Germany: Springer-Verlag, 1972.

Predrag R. Jelenković (S'94–A'95) was born in Kraljevo, Serbia, in 1966. He received the B.S. degree from the University of Belgrade, Serbia, in 1991, and the M.S., M.Ph., and Ph.D. degrees from Columbia University, New York, in 1993, 1995, and 1996, respectively, all in electrical engineering.

During the summers of 1993 and 1994 he worked at C&C Research Laboratories, NEC USA, Inc., and AT&T Bell Laboratories, respectively. For his summer work at NEC, he was awarded the NEC Patent Award in 1996. He joined the Mathematics of Networks and Systems Department, at Bell Laboratories, Lucent Technologies, in October 1996, as a Member of Technical Stuff. His research interests include mathematical modeling, analysis, and control of computer communications networks and systems.

As a graduate student, he received in 1993 the Edwin Howard Armstrong Memorial Award for superb academic record, and in 1996 the Eliahu I. Jury Award for excellence in the area of Systems, Communications and Signal Processing.

Aurel A. Lazar (S'77–M'80–SM'90–F'93) is a Professor of Electrical Engineering at Columbia University, New York, NY. His research interests span both theoretical and experimental studies of telecommunication networks and multimedia systems. The theoretical research he conducted during the 1980's pertains to the modeling, analysis, and control of broad-band networks. He formulated optimal flow and admission control problems and, by building upon the theory of point processes, derived control laws for Markovian queueing network models in single-control as well as game-theoretic settings. He was the chief architect of two experimental networks, generically called MAGNET. This work introduced traffic classes with explicit quality of service constraints to broad-band switching, and led to the concepts of schedulable, admissible load, and contract regions in real-time control of broad-band networks. In the early 1990's, his research efforts shifted to the foundations of the control, management, and telemedia architecture of future multimedia networks. His involvement with gigabit networking research led to the first fully operational service management system on ATM-based broad-band networks. The system was implemented on top of AT&T's XUNET III gigabit platform spanning the continental U.S. His management and control research pioneered the application of virtual reality to the management of ATM-based broad-band networks. His current research in broad-band networking with quality of service guarantees focuses on modeling of video streams and analyzing their multiplexing behavior, with emphasis on multiple time scales and subexponentiality. He is also leading investigations into multimedia networking architectures supporting interoperable exchange mechanisms for interactive and on-demand multimedia applications with quality of service requirements. The main focus of this work is on building a broad-band kernel (also known as **xbind**) that enables the rapid creation, deployment, and management of multimedia services. Resource allocation and networking games algorithms form the core of this architecture. He was instrumental in establishing the OPENSIG international working group, with the goal of exploring network programmability and next-generation signaling technology.

Nemo Semret received the B.Eng. degree (Honors) in electrical engineering with minor in mathematics with "Distinction" and a "University Scholar" designation, and the M.Eng. degree in electrical engineering from McGill University, Montreal, P.Q., Canada. He is currently working toward the Ph.D. degree in electrical engineering at Columbia University, New York.

His most recent job was in the Multimedia Communications Research Department of Bell Labs, Murray Hill, NJ. He has worked as a Consultant for the UNECA on low-cost electronic mail, as a Research Staff Member at INRS-Télécom developing speaker recognition software, has interned at Intelsat, the National Research Council of Canada's Dominion Radio-Astrophysical Observatory, and the McGill Center for Intelligent Machines. He is the author of a Java program which was rated in the top ten on the WWW in 1996. His current research interests are in game-theory, design of network resource control and management mechanisms, video traffic-modeling, and distributed algorithms.